Boulder Atmosphere Innovation Research

Boulder A.I.R. L.L.C; 2820 Lafayette Dr., Boulder, CO 80305, U.S.A.; dh.bouldair@gmail.com

March 27, 2021

To:

City of Longmont
350 Kimbark Street
Longmont, CO 80501

Attn: Dr. Jane Turner

Re: Longmont Regional Air Quality Study – Year 2020 Quarter 4 Report

Dear Dr. Turner,

Please find included with this letter the October – December (Quarter 4) 2020 report for our work on the Longmont Air Quality Study. The monitoring data and data interpretations are presented.

Thank you for providing this opportunity for air quality monitoring to Longmont citizens and the City of Longmont. We would be happy to discuss any questions that you, other City staff or Longmont citizens may have.

Sincerely,

Detlev Helmig

Detlev Helmig

Boulder AIR LLC

2020 Quarter 4 (October – December) Report

Longmont Air Quality Study

Executive Summary

This report summarizes the data and preliminary findings from the Longmont Air Quality Study during October through December of 2020. All variables were reported in near-real time on the public *Longmont Air Quality Now* web portal.

This report includes graphical analyses of all data acquired during October-December, i.e. quarter 4 (Q4), 2020. In addition, data comparisons and analyses of selected events that resulted in enhanced concentrations are presented. LMA and LUR data are compared with each other and also with concurrent observations from the Boulder Reservoir and the Broomfield Soaring Eagle Park and Livingston sites.

Notable events during Q4 were one exceedance of the ozone National Ambient Air Quality Standard (NAAQS) in early October, which was remarkably late in the year for such a high ozone day. Smoke plumes originating from wild fires in California caused a number of days with high particulate matter loadings. The 24-hour PM2.5 NAAQS was exceeded on four days during this event.

Occurrences of elevated oil and gas tracer concentrations, as observed in Q1 of 2020, were less frequent and less elevated. Q4 data provide additional support for the hypothesis presented in the Q3 report; specifically, that emission reductions from oil and gas operations in the vicinity (estimated at a few miles) of LUR occurred and were sustained during and after spring of 2020.

Table of Contents

1. Project Scope and Goals

No changes from Q3 report.

2. Overview of the Monitoring Program

No changes from Q3 report.

3. Air Quality Monitoring Study Updates

No changes from Q3 report.

4. Data Quality Assurance/Quality Control Process

No changes from Q3 report.

5. Website Development

We added 3-day and 30-day graphs of additional compounds to the website. These graphs can be accessed through a new link at the bottom of the 3-Days Graphs and 30-Day Graphs pages. With these additions, the currently plotted volatile organic compounds (VOCs) are ethane, propane, i-butane, n-butane, acetylene, benzene, toluene, ethane, propene, cyclopentane, i-pentane, n-pentane, isoprene, n-hexane, n-heptane, n-octane, ethyl-benzene, m/p-xylene, o-xylene. In addition, there is one graph displaying the i/n-pentane ratio.

6. Data Archiving

No Changes from Q3 report.

7. Data for Quarter 4, 2020

The data that were recorded in Q4, 2020, are included in this report in graphical time series format in Supplement A (LMA) and Supplement B (LUR). These graphs provide the records of the completeness of the data coverage and general features in the dynamic, diurnal, and seasonal changes. Some of the data (e.g. wind direction) are difficult to interpret when 3 months of data are included in the same plot. In these instances, the primary objective is to show general trends and that the data are nearly continuous – not to point out individual features. Data coverage for all variables is >95% for the full quarter.

In Supplement C, the variables that are measured at both sites are shown together in a set of time series graphs. These graphs are presented to highlight similarities and differences between the two locations.

8. Selected Data Examples and Preliminary Interpretations

Ozone

The full Q4 ozone records for LMA and LUR are presented in Figures SA8 and SB8.

The 8-hour ozone National Air Quality Standard (NAAQS) was exceeded at LMA on October 8, with a maximum 8-hour averaged ozone value reached of 71.3 ppb (Figure SA9). The maximum 8-hour value at LUR on this day was 68 ppb. This is an unusual occurrence because the 'ozone season' is typically regarded as May – August. According to the Denver/Boulder NWS records (NWS Boulder Denver Daily Normals and Records October (weather.gov)), October 8 had a record high of 85° F, 16° F above normal. Skies were clear in the afternoon and there was a 500-mb ridge over Colorado. Combined with the warm temperatures, these factors are typical for summer-time high ozone events along the Front Range.

Figure 1 presents a statistical analysis of the full Q4 ozone data, comparing the Longmont data with observations from BRZ and BSE. This analysis illustrates the increasing difference in the ozone distribution between the sites, with ozone at LUR becoming lower towards the winter months. This trend is predominantly driven by a reversal of nitrogen oxides (NO_x) - ozone chemistry moving from the summer to winter. During winter, with lower levels of solar irradiance, and shorter daytime hours with less light overall available throughout the daytime hours to fuel photochemistry, emissions of nitrogen oxides mostly reduce ozone by reaction of nitric oxide with ozone. The lower ozone levels seen at LUR in comparison to the other monitoring stations reflect a relatively stronger rate of ozone destruction from reaction with nitric oxide. This is indicative of higher levels/emissions of nitric oxide at LUR, which is confirmed by the NO_x monitoring results (see below).

CO_2

The full Q4 CO_2 records are available in Figures SA6 and SB6 for LMA and LUR, respectively. The statistical comparison of the monitoring data is presented in Figure 2. The wind speed/wind direction analyses are shown in Figure 3. It is striking that the relative enhancement of CO_2 at LUR increased from Q3 to Q4, and that the differences between LUR and the comparison sites became progressively greater towards the end of the year. Clearly, LUR is subjected to the strongest CO_2 emissions. The increasing difference is likely due to emissions from nearby sources being trapped near the surface as the frequency and strength of temperature inversions, resulting in a shallow layer of stable air at the surface, increase in winter. The results from the wind direction/speed analysis are similar to those reported in the preceding quarters (Figure 4), with possibly a somewhat stronger contribution from the east during Q4. Again, LMA shows a relatively strong CO_2 source to the west of the site. This is surprising as there is mostly open, undeveloped land to the west of the airport, while development and traffic is much stronger to the east. We are in the process of investigating the possible source of the CO_2 transport from this sector. Two possibilities are currently being analyzed. There are eight small aircraft hangers to the west of the monitoring site. According to information obtained from the airport manager, several of those are heated by natural gas furnaces. The exhaust from these furnaces could possibly be a source of the CO_2. Another possibility is the Cemex cement plant that is located approximately 3 km to the northwest of the monitoring station. CO_2 is emitted as a waste product as limestone is heated for production of cement.

Q4 is the first quarter where we can compare the seasonal monitoring results from one year to another. Figure 5 and Table 1 provide this 2020-2019 CO_2 data comparison. These data must be considered against the global increase in CO_2, which was approximately 2.5 ppm during this one-year time window. Over 25,000 individual 5-min annual data points were considered in the comparison. Interestingly, there was a slight decrease in the mean and median CO_2. Overall, the pattern observed is that lower percentile values increased slightly, while upper percentile values decreased. This behavior in the data suggests that local CO_2 sources that influence CO_2 at the site could have been weaker in 2020 compared to 2019. However, these differences may have been caused by differences in meteorology during these two years. Additionally, a decrease in CO_2 emissions due to COVID lockdowns may have been a contributing factor. With each quarter we will obtain additional data points to further expand this analysis.

Methane

The full Q4 methane records are available in Figures SA7 and SB7 for LMA and LUR, respectively. Similar to what was already described for CO_2, the relative difference in the statistical distribution of methane between the sites increased during Q4, probably for the same reasons (Figure 6). LUR had the highest methane percentile values at each level and for each month during Q4. The wind dependency of elevated methane is about the same as during the preceding quarters (Figure 7). For both sites, transport from the north to east are the predominant source sectors.

The Q4 2020 versus 2019 comparison of methane at LMA is presented in Figure 8. Numerical results of this analysis are included in Table 1. These data need to be interpreted against the approximately 7 ppb increase in the northern hemispheric methane background during this time window. The methane increases seen in the data are quite inconsistent, spanning from -89 ppb to 86 ppb at the different percentile values. The mean and median values are both below the global methane trend. The variability in the data, expressed by the standard deviation, was about the same between both years (98.7 versus 95.2 ppb). With this behavior seen in the data it is too soon to make any definite statements about possible changes in methane sources that exert an influence on the recordings from the site.

VOCs

The full Q4 LUR records for six selected VOCs are available in Figures SB10–SB16. Figure 9 presents the full year 2020 record of ethane, benzene, and acetylene. These graphs allow further elucidating the drops in the oil and gas tracers that were discussed in detail in the Q3 report. Of the three, the acetylene data display a more typical seasonal behavior for VOCs emissions with a higher frequency and higher maximum concentrations during winter/spring, lower values during the summer, and then increasing levels again during fall/winter. This behavior is quite typical, and mainly reflects the seasonal changes in atmospheric mixing/dilution, which follow the annual seasonal solar cycle. During summer, with longer daylight hours, and higher maximum daytime solar radiation levels, there is more solar heating that drives thermal convection, boundary layer growth, and atmospheric mixing, which causes dilution of surface emissions. The lower summer values are the result of these factors. The ethane and propane annual cycles observed are quite different. While there is a slight increase towards the 2020 fall/winter, concentration values fall well short of the values seen during spring. This behavior solidifies the hypothesis that oil and gas emissions in the immediate surrounding of the monitoring station (estimated to be a few miles) remained lower from mid-spring onwards to the end of the year than what was observed at the onset of the monitoring program (February to early April).

The statistical comparison of the VOCs plotted in Figure 10 shows again how VOCs are overall higher at LUR in comparison to the other sites. This now also applies to benzene, which had shown a possible trend towards lower levels (than the other sites) during Q3. Wind speed/wind direction dependence of ethane, propane, acetylene, and benzene is similar to Q3 (Figure 11). VOC-VOC analyses show somewhat tighter correlations than in the preceding quarter (Figure 12), which likely is, at least partially, driven by the overall higher concentrations.

The analysis of VOCs signatures, using VOC/VOC ratio values, shown in Figure 13, includes a new analysis graphic: the ratio of i/n-butane. Butanes are mostly associated with natural gas. Two of their more common uses are as fuel in cigarette lighters or camping fuel. The ratio of the two butane isomers in the atmosphere is relatively well defined, and shows a relatively low variability, with most values falling between 0.4 – 0.6. The results from the LUR analysis are quite remarkable. There is a very clear difference in the i/n-butane ratio in air arriving from the different sectors. Air originating from the northeast has lower values, on average ~0.35, whereas air transported from the southwest sector has a signature of ~0.55. These differences likely reflect a unique signature of the butanes that are emitted from the regional Denver Julesburg Basin petroleum reservoir that contrasts the butane ratio in natural gas distributed through the city utilities. For both sectors, the signature values become more defined at higher wind speeds. These new analyses add another piece of evidence that underscores the very different chemical nature of air being transported to Longmont from the northeast to east versus the western sectors.

Nitrogen Oxides (NO, NOx)

The Q4 LUR record for nitric oxide (NO) is available in Figure SB17, and the record for NO_x in Figure SB18. NO and NO_x levels increased steadily from October to November to December. Both NO and NO_x were significantly higher, approximately a factor of 2-3, at LUR compared to the Boulder Reservoir and the Broomfield Soaring Eagle Park (Figure 14). Dependency of NO and NO_x on wind direction and wind speed is presented in Figure 15.

Particulate Matter (PM)

PM10 and PM2.5 LUR Q4 monitoring results are presented in Figure SB19 and SB20. The 24-hour averaged PM2.5 data, in comparison to the NAAQS threshold value, are available in Figure SB21. The comparison of LUR data with BSE is presented in Figure 16. While the seasonal trends are quite similar for both sites, recordings at LUR are on average 10-20% higher. There were a number of days in early October with highly elevated levels of particulates, resulting from wild fire smoke plumes transported into the Colorado Front Range. The 24-hour PM2.5 air NAAQS was exceeded on four days, i.e. October 8, 10, 16, and 17. The highest value, at 64.8 $\mu g\ m^{-3}$, was recorded on October 17. The smoke originated from wildfires in northern California and covered a wide geographical area in the western United States, as can be seen from the archived NOAA smoke data map shown in Figure 17.

Tables

Table 1:
Comparison of the statistics of CO_2 and methane data (5-min averages) at LMA during Q4 of 2020 and Q4 of 2019.

LMA CO2 & CH4, Q4 Yearly Statistics

species	stat	2019	2020	Abs Diff	% Diff
CH4 (ppb)	count	25133	26348	1215	4.0
CH4 (ppb)	mean	2051.0	2053.5	2.5	0.1
CH4 (ppb)	std	95.2	98.7	3.5	3.7
CH4 (ppb)	min	1820.9	1907.0	86.1	4.7
CH4 (ppb)	5%	1933.3	1951.1	17.8	0.9
CH4 (ppb)	25%	1986.6	1985.9	-0.7	-0.0
CH4 (ppb)	50%	2033.9	2029.7	-4.2	-0.2
CH4 (ppb)	75%	2096.3	2090.4	-5.9	-0.3
CH4 (ppb)	95%	2222.0	2235.9	13.9	0.6
CH4 (ppb)	max	3079.0	2990.4	-88.6	-2.9
CO2 (ppm)	count	25133	26348	1215	4.0
CO2 (ppm)	mean	428.8	427.3	-1.5	-0.3
CO2 (ppm)	std	14.4	12.5	-1.9	-13.1
CO2 (ppm)	min	386.8	408.1	21.3	5.5
CO2 (ppm)	5%	409.8	411.5	1.7	0.4
CO2 (ppm)	25%	417.0	417.9	0.9	0.2
CO2 (ppm)	50%	427.0	425.4	-1.6	-0.4
CO2 (ppm)	75%	438.1	434.2	-3.9	-0.9
CO2 (ppm)	95%	454.5	449.6	-4.9	-1.1
CO2 (ppm)	max	621.4	521.1	-100.3	-16.1

Figures

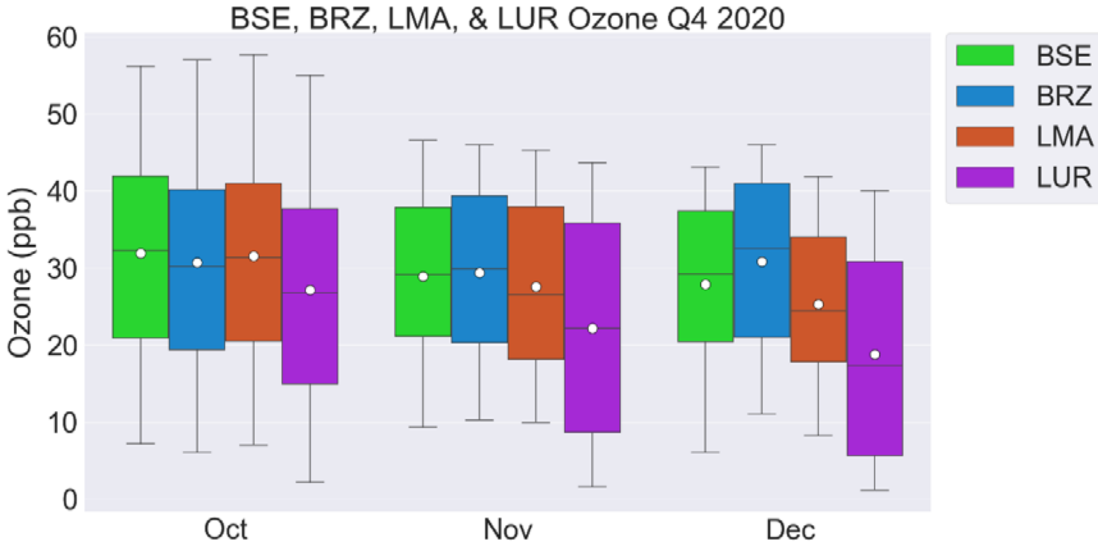

Figure 1:
Comparison of the ozone distribution at BSE, BRZ, LMA, and LUR during Oct – Dec 2020. These box whisker plots show the median value as the center line, the 25-75 percentile distribution as the colored boxes, and the 5-percentile and 95-percentile values as the whiskers. The white dot on each box illustrates the mean value at each site. Ozone at LUR showed the overall lowest percentile values, followed by LMA. These differences are mostly driven by higher levels of nitrogen oxides at the Longmont sites. Nitric oxide, particularly in the winter, is a sink of ozone at low light conditions (nighttime hours).

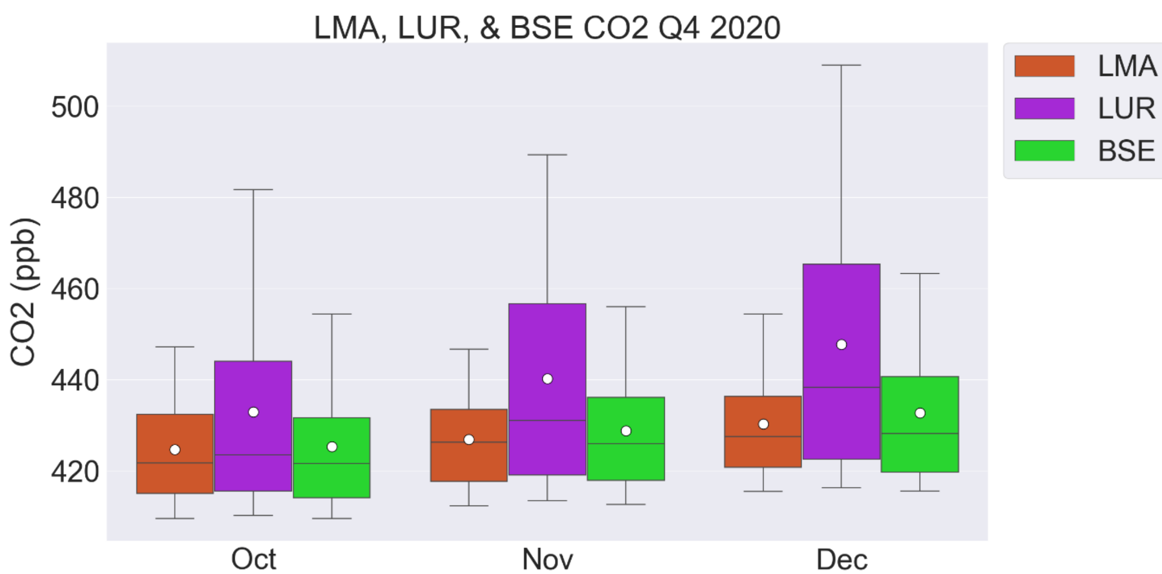

Figure 2:
Comparison of the CO_2 distribution at LMA, LUR, and BSE during Oct – Dec 2020. See Figure 1 for explanation of the box whisker plot format. LUR had the overall highest variability and highest CO_2 percentile values among these three sites, likely indicating the strongest CO_2 sources in the vicinity of the LUR station.

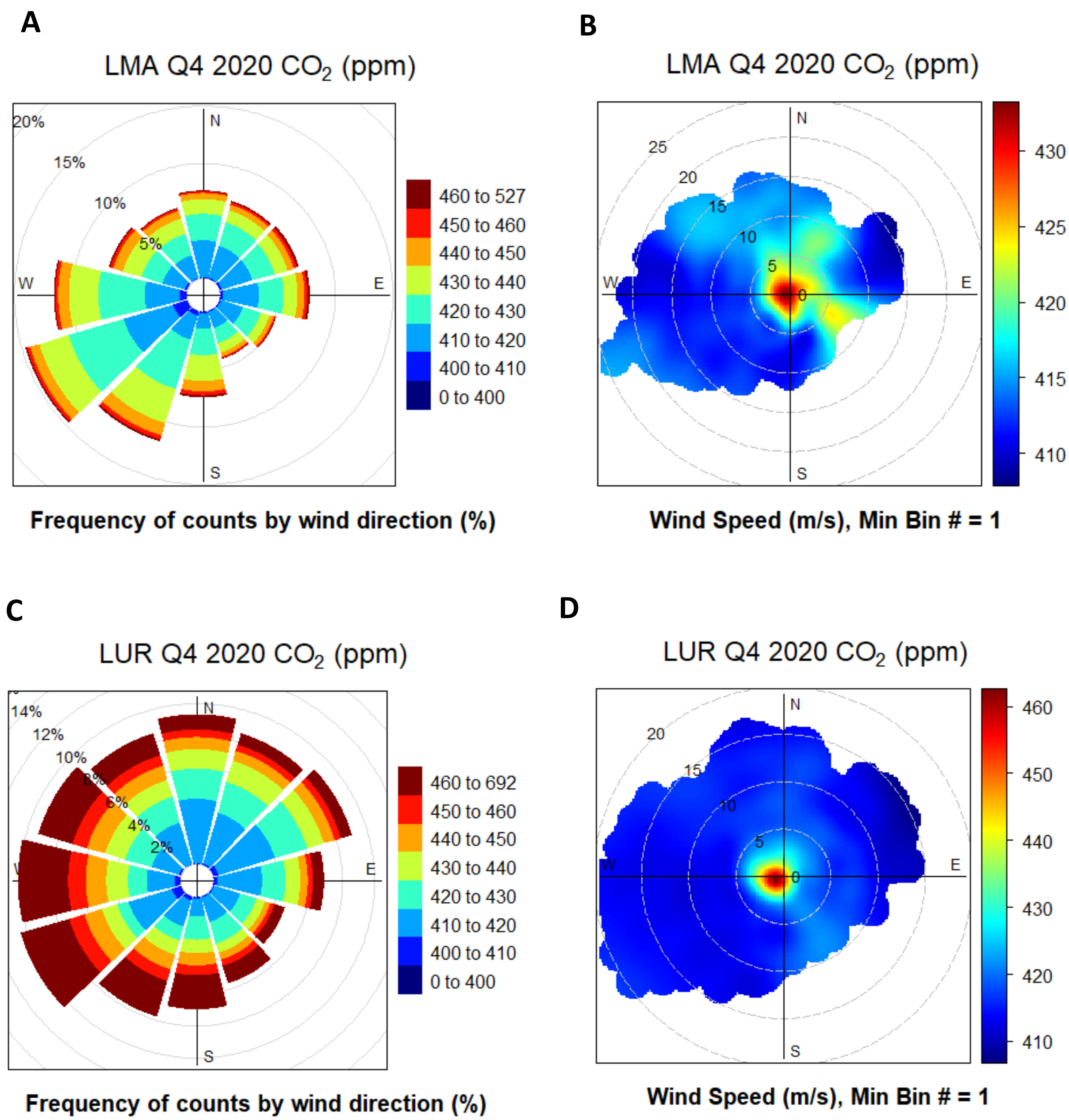

Figure 3:
Wind rose (left) and wind heat map analysis showing the dependency of CO_2 mole fractions at LMA (top, A, B) and LUR (bottom, C, D) during Oct – Dec 2020. These results are similar to the ones reported in the two previous quarterly reports. The LUR site is east of the City of Longmont. These analyses suggests that the city is the primary source for enhanced CO_2 observed at LUR. The cause for the high CO_2 mole fractions seen in winds from the west of LMA is surprising. These data suggest that a cement plant to the northwest of the station could be a potential source of CO_2 emissions.

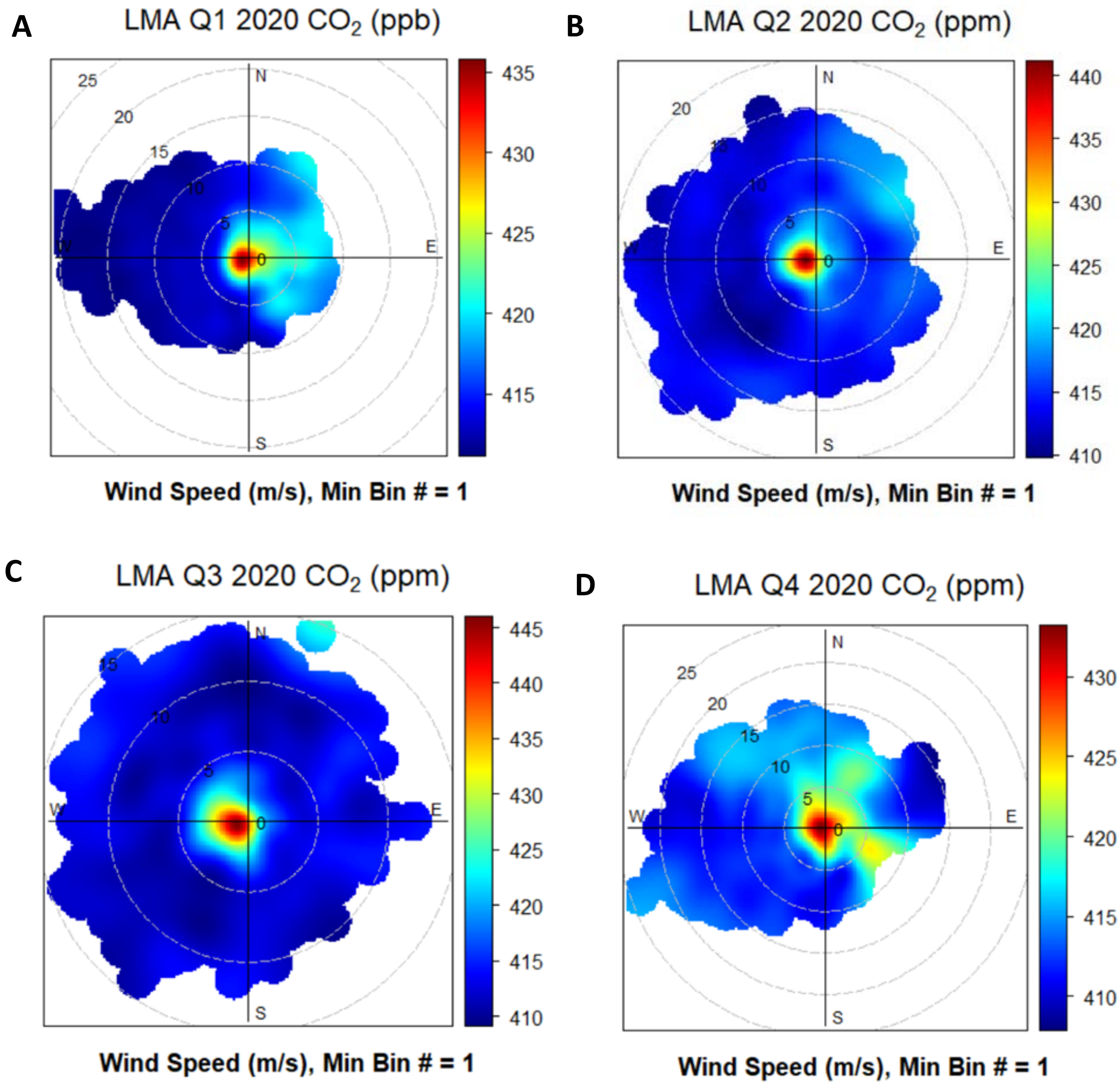

Figure 4:
Comparison of the wind speed/wind direction to observed CO_2 at LMA during Q1-Q4 of 2020. There is a consistent pattern with a relatively strong source to the west of the station throughout the year.

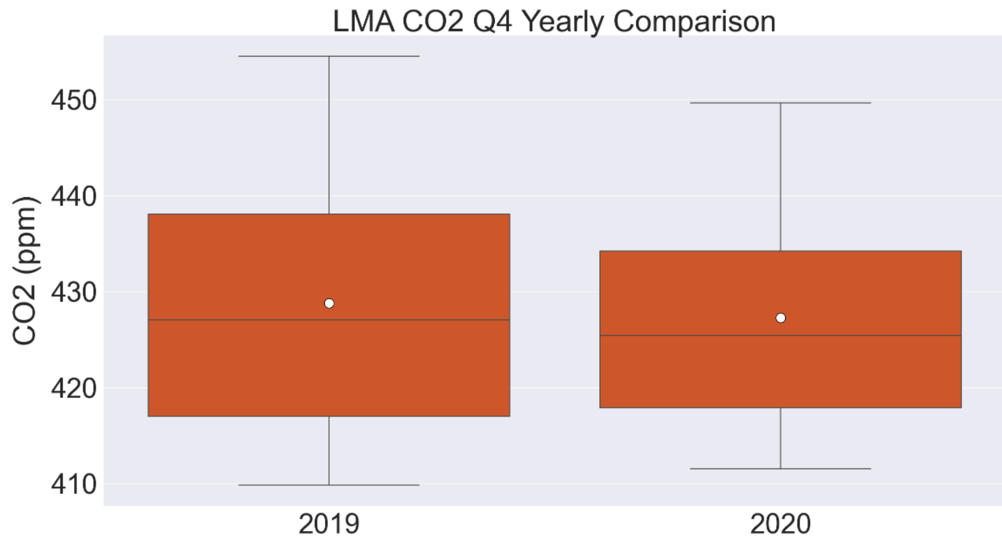

Figure 5:
Comparison of the CO_2 distribution at LMA during Q4 of 2019 and 2020. See Figure 1 for explanation of the box whisker plot format. While the lower percentile values show a slight increase from 2019 to 2020, higher percentile values were slightly lower (see Table 1 for the numerical values). This could be interpreted as a lower number of occurrences of conditions with highly elevated CO_2.

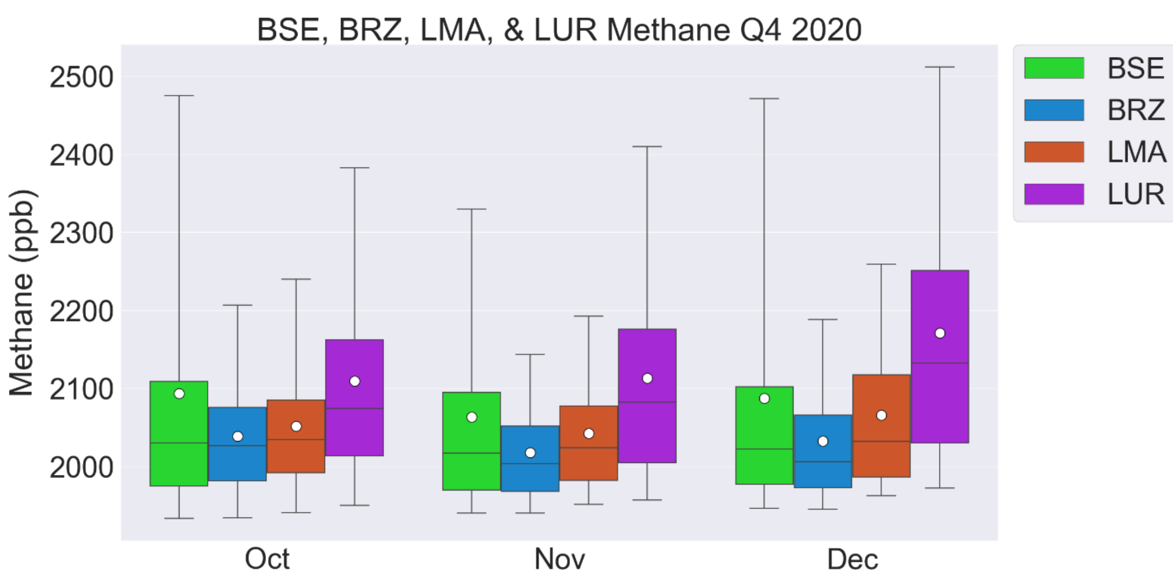

Figure 6:
Comparison of the methane distribution at BSE, BRZ, LMA, and LUR during Oct – Dec 2020. See Figure 1 for explanation of the box whisker plot format. Similar to the previous quarters, LUR recorded more variability and larger values at the higher percentile margins. Among the two Longmont sites, LUR has higher absolute values and variance when compared with LMA.

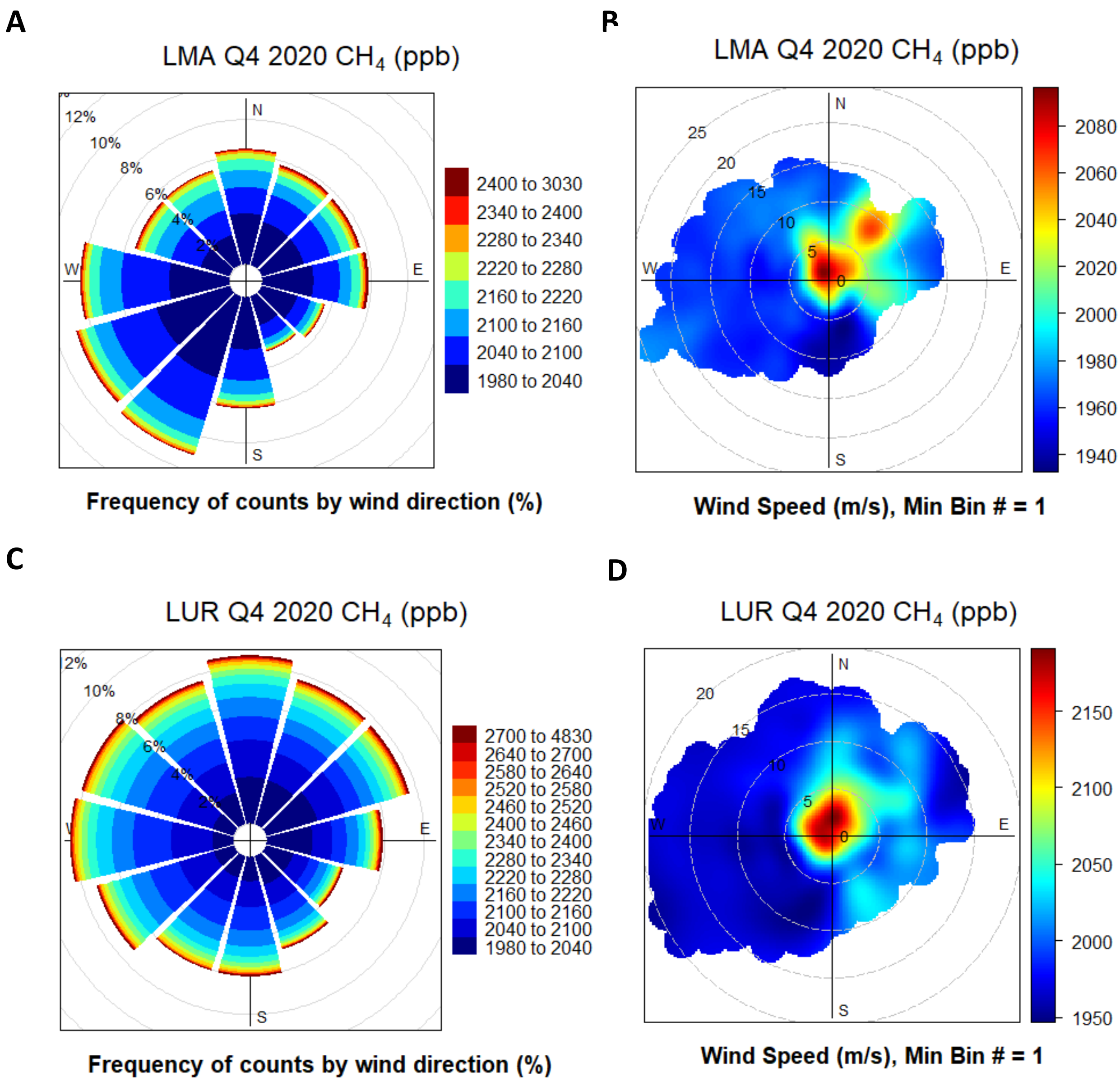

Figure 7:
Wind rose (left) and wind heat map analysis showing the dependency of CH_4 mole fractions at LMA (top, A, B) and LUR (bottom, C, D) during Oct – Dec 2020. High methane values are primarily transported from the north to northeast sector at LUR. LMA shows a relatively stronger contribution from the north.

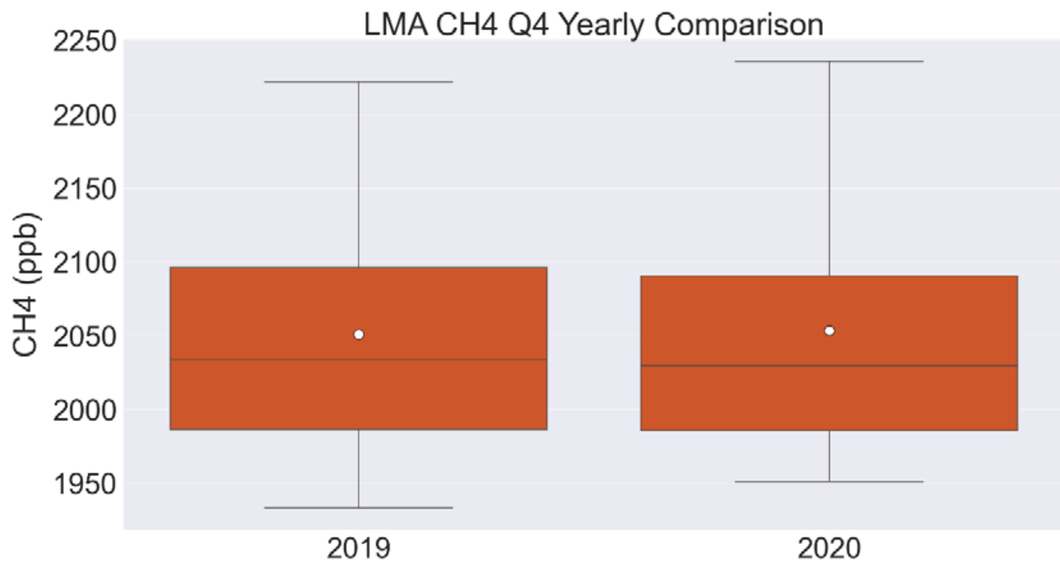

Figure 8:
Comparison of the methane distribution at LMA during Q4 of 2019 and 2020. See Figure 1 for explanation of the box whisker plot format. The numerical values for the statistical distributions are presented in Table 1. While these box-whisker plots are barely distinguishable, there was a slight increase in the lower percentile values and mostly a slight decrease in the higher percentile values.

Figure 9:
Ethane (A, top), benzene (B, middle), and acetylene (C, bottom) at LUR between late January and December 31, 2020. Lower frequency and lower maximum values of concentration spikes during the summer are observed for all three compounds. These summer minima are mostly caused by the stronger mixing (dilution) of surface air from thermal convection. For acetylene, a compound that is mostly the result of combustion, similar peak patterns are observed for spring and the fall-winter of 2020. The behavior of the oil and gas tracer ethane is quite different. Here, occurrences of spikes are overall lower in the fall-winter. A similar pattern is observed for benzene. These features suggest that there has been a shift (decline) in the source strength for these two compounds towards the latter part of the year.

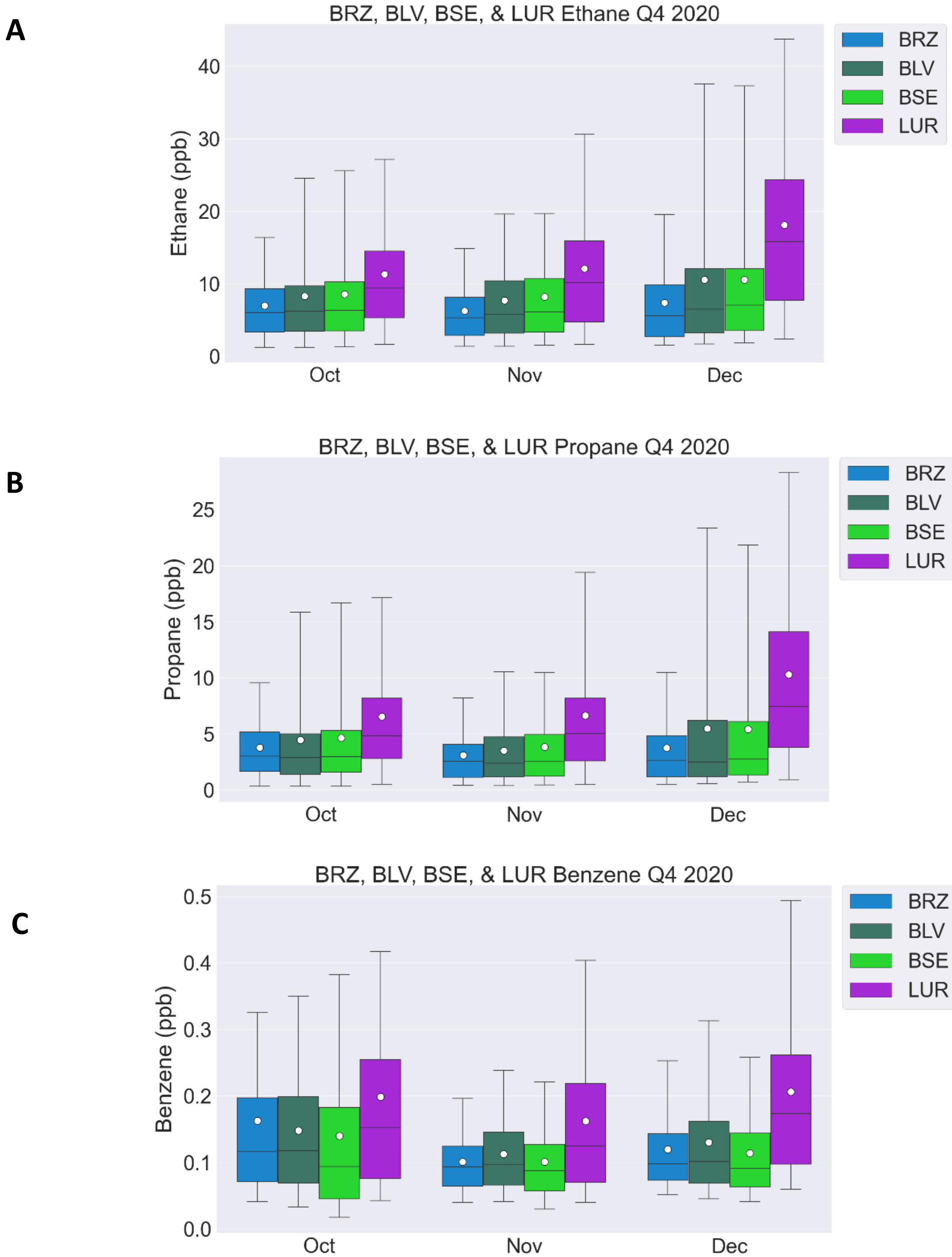

Figure 10:
Comparison of the distribution of ethane (A), propane (B), and benzene (C) at BRZ, BLV, BSE, and LUR during Q4. See Figure 1 for explanation of the box whisker plot formats. A pattern seen during Q3 appears to be continuing: For the oil and gas tracers ethane and propane, the higher percentile values at LUR appear to be increasing at higher rates than at BRZ and BSE.

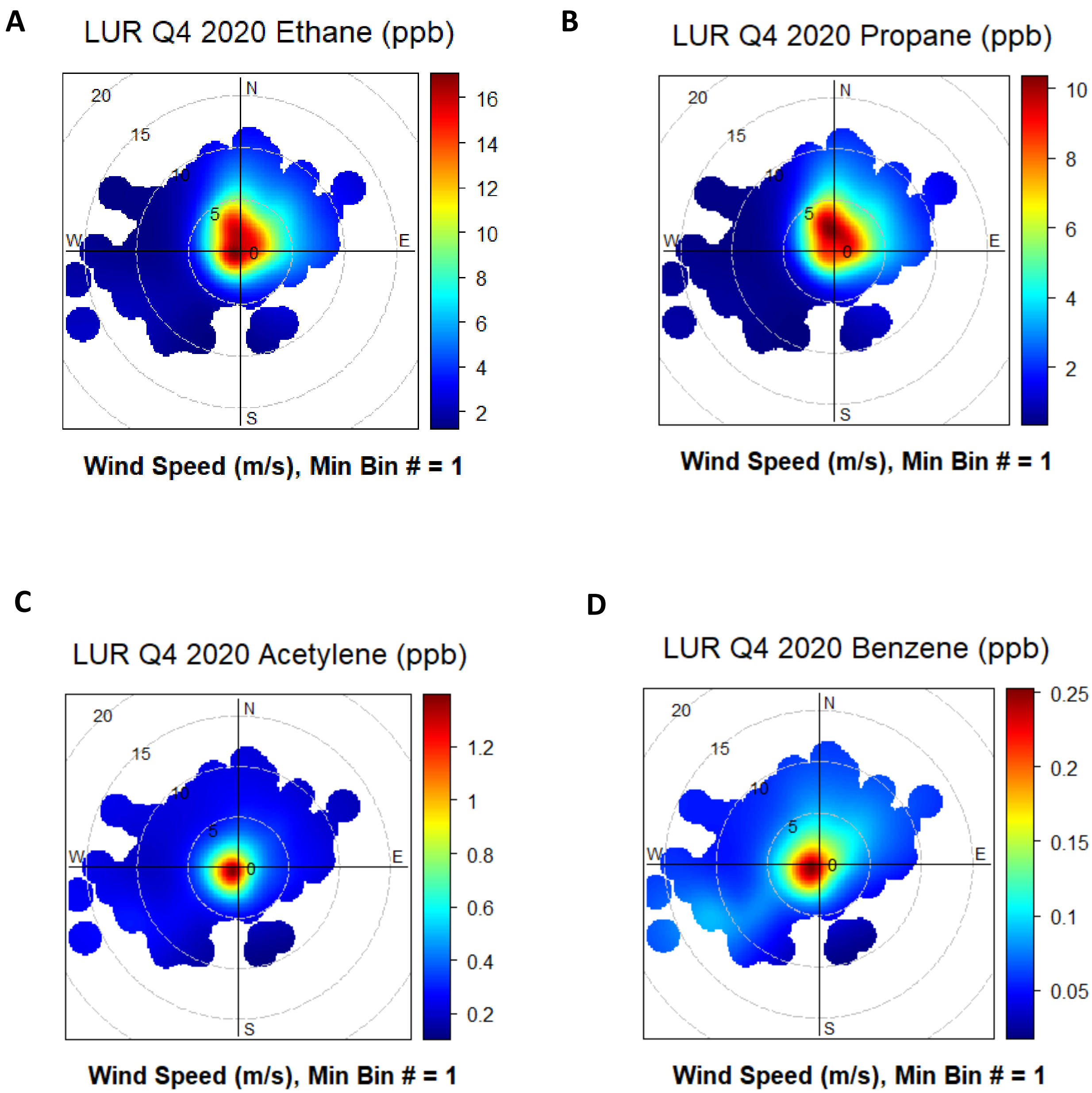

Figure 11:
Comparison of ethane (A), propane (B), acetylene (C), and benzene (D) occurrences as a function of wind speed and direction at LUR during Q4. These results are similar to those reported in Q3.

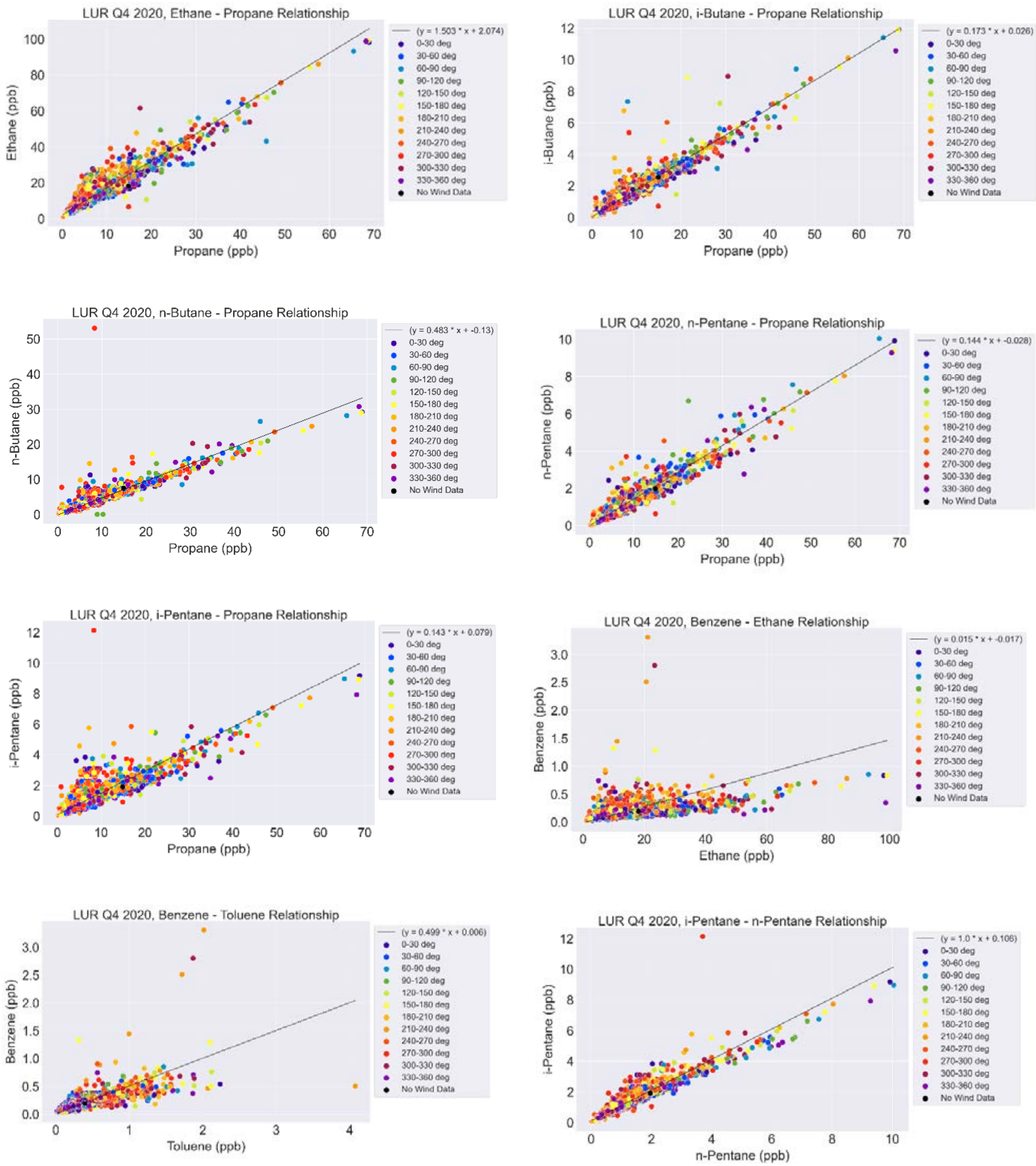

Figure 12:
VOC-VOC relationships at LUR during Q4. Data points are color coded by wind direction. The black line is an orthogonal linear best fit regression calculation. The overall wider distribution and higher values compared to Q3 allow for a better definition of these relationships.

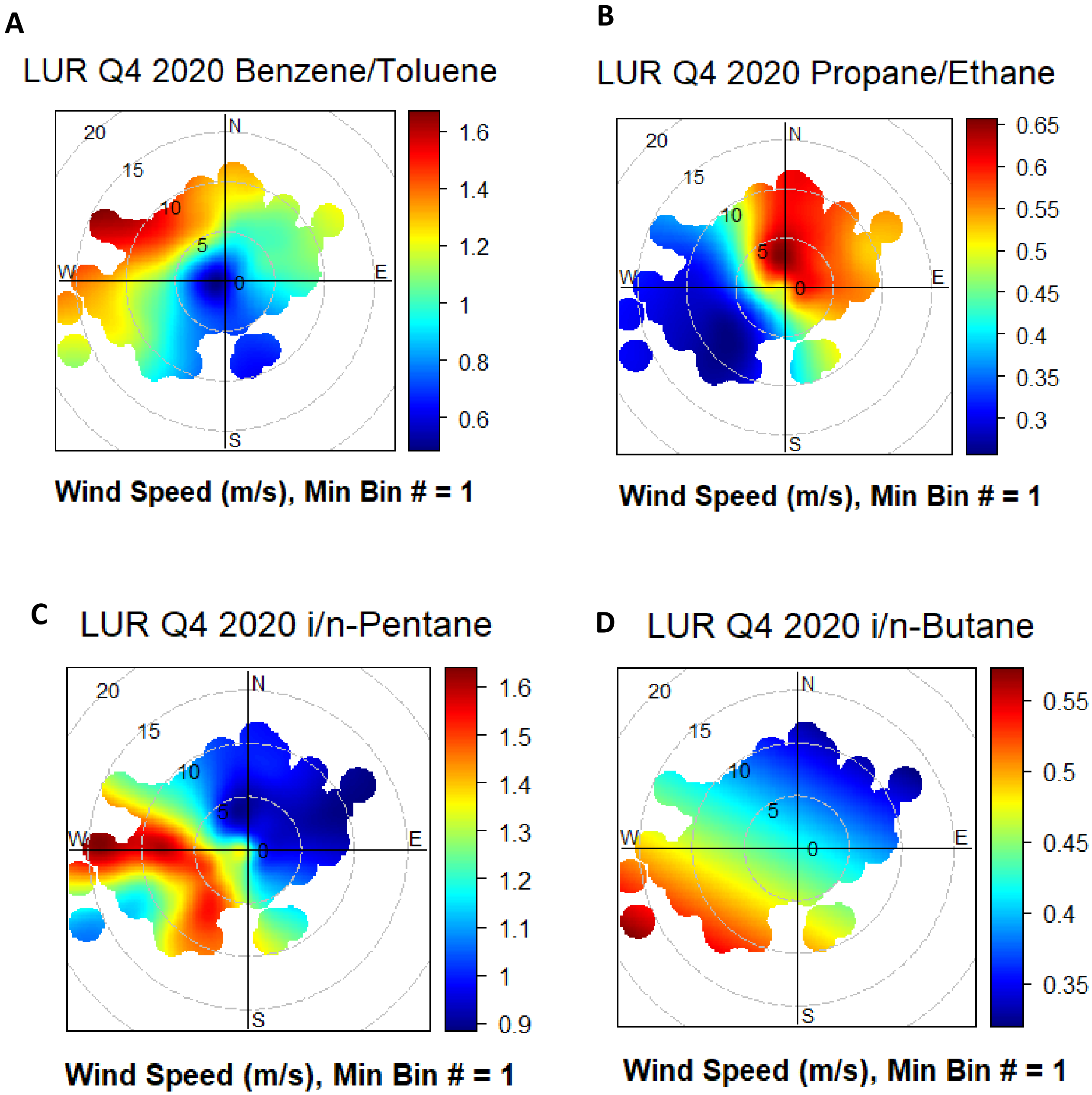

Figure 13:
Ratios of selected VOC pairs as a function of wind direction and wind speed during Q4. These analyses mostly confirm the patterns that were first reported in Q3, with one exception, which is the lack of a high benzene source in the northeast sector that was prominent feature in the Q3 data.

A

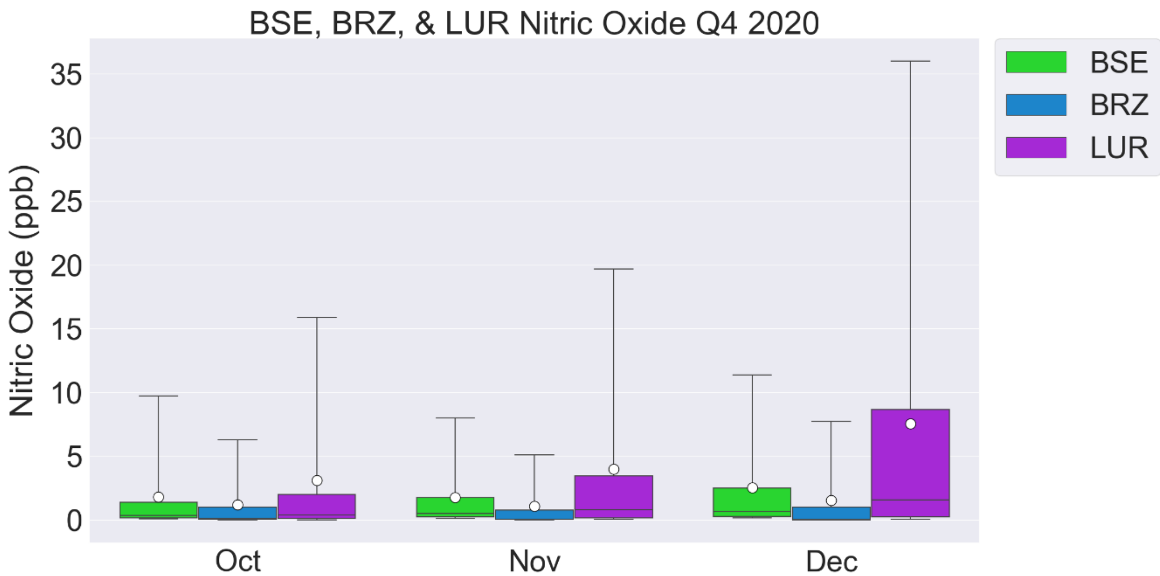

B

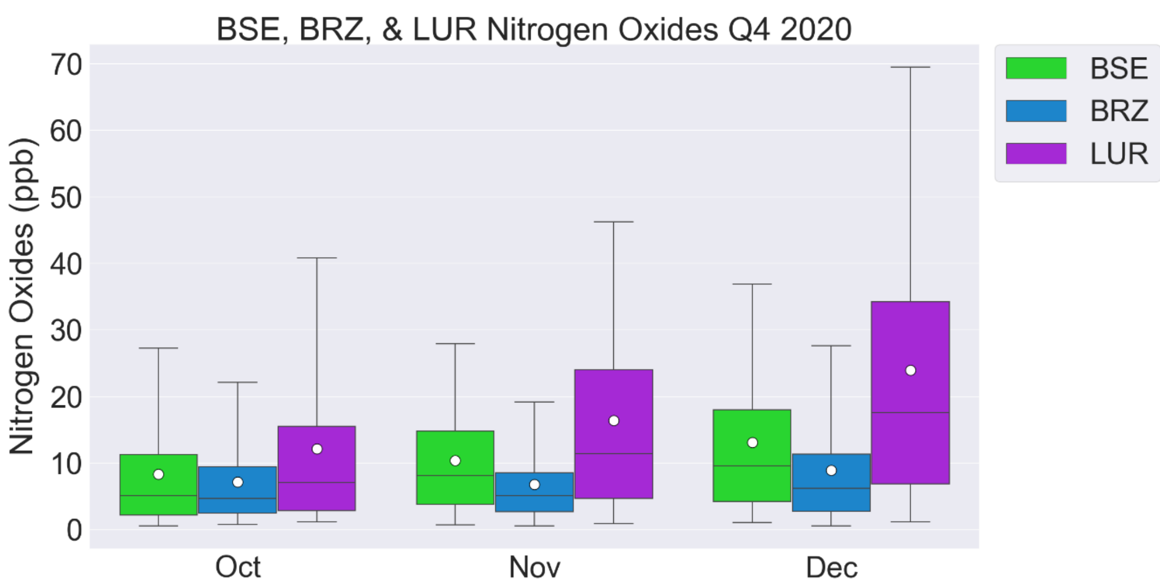

Figure 14:
Comparison of nitric oxide (A) and nitrogen oxides (B) at BSE, BRZ, and LUR during Oct – Dec 2020. See Figure 1 for explanation of the box whisker plot formats. These data continue a pattern seen previously, at now even higher clarity: NO and NO_x mole fractions, and the variability in the data are higher at LUR than at sites in neighboring cities.

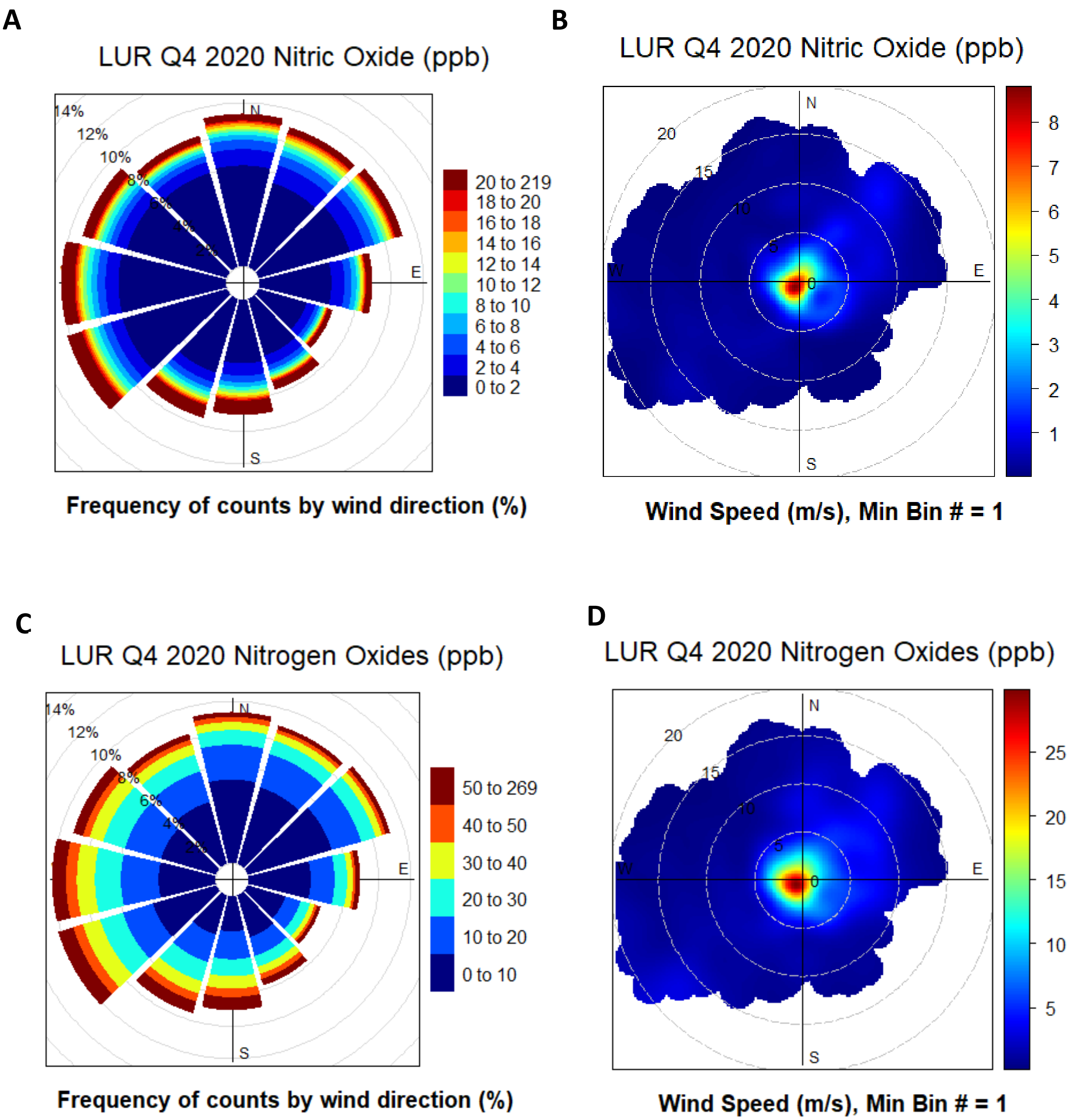

Figure 15:
Dependence of nitric oxide (A, B) and nitrogen oxides (C, D) as a function of wind speed and direction at LUR during Oct - Dec 2020. As seen in the prior data, the City of Longmont, located to the west, appears to be the strongest upwind source for NO_2. NO results are not quite as well defined.

A

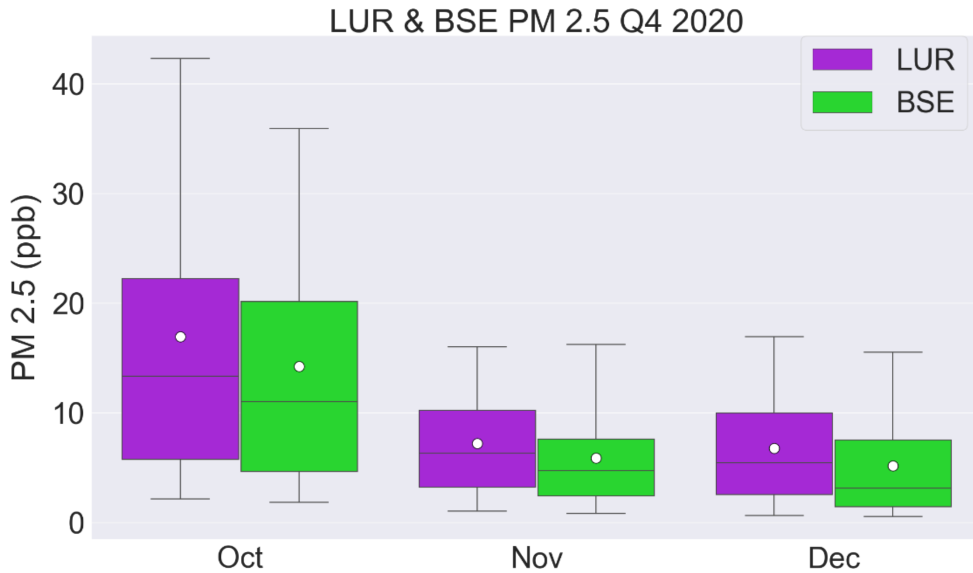

B

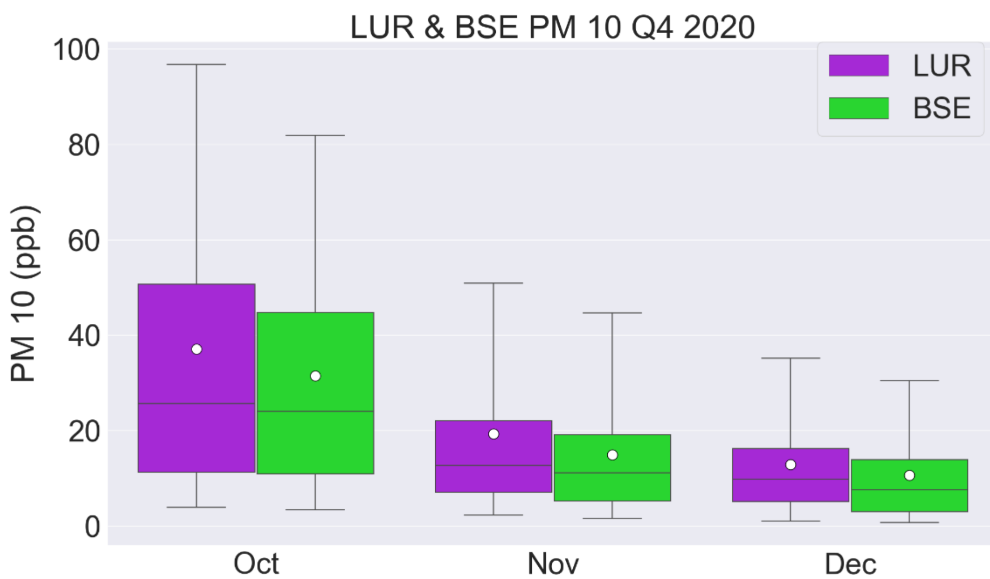

Figure 16:
Comparison of PM 2.5 (A) and PM 10 (B) at LUR and BSE during Oct - Dec 2020. See Figure 1 for explanation of the box whisker plot formats. A similar seasonal trend is observed for both sites. Particulate concentrations are slightly higher at LUR compared to BSE.

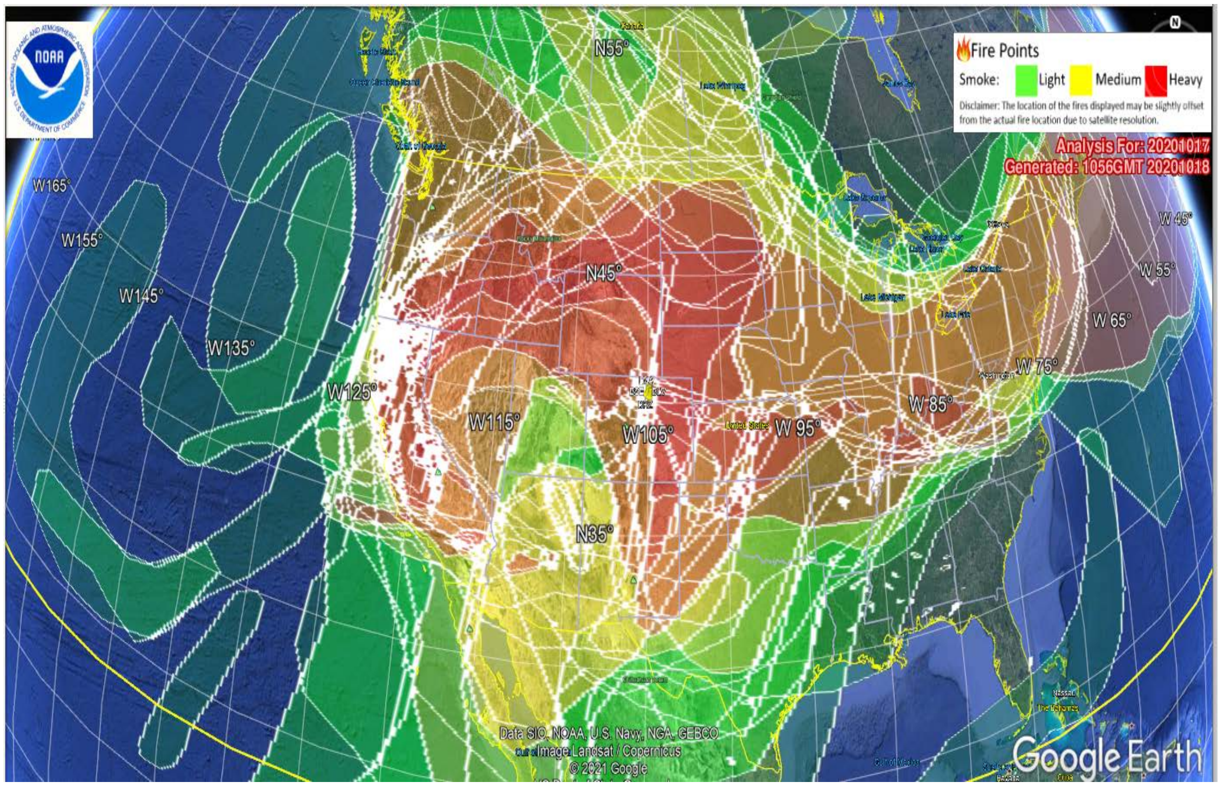

Figure 17:
Smoke transport over the United States on October 17, 2020, when the Q4 maximum PM2.5 concentration was recorded at LUR. Map was retrieved from the NOAA smoke forecasting system at https://www.ospo.noaa.gov/Products/land/hms.html#0.

Supplement A

Preliminary Data LMA Quarter 4, 2020

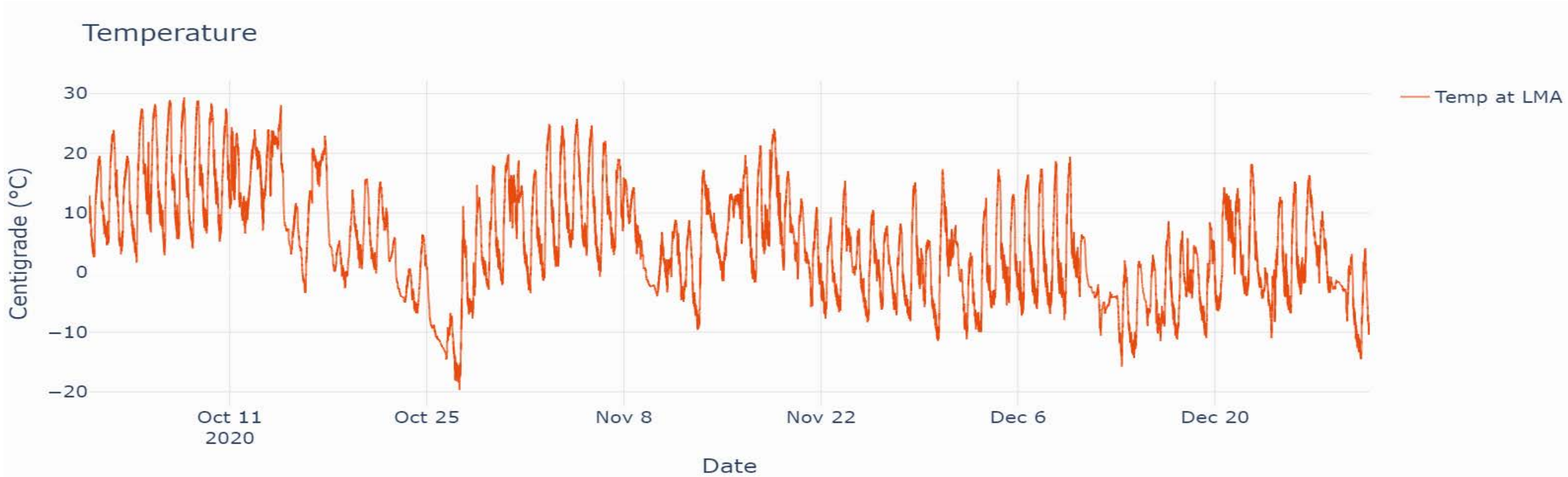

Figure SA1:
LMA temperature record Oct 1 – Dec 31, 2020.

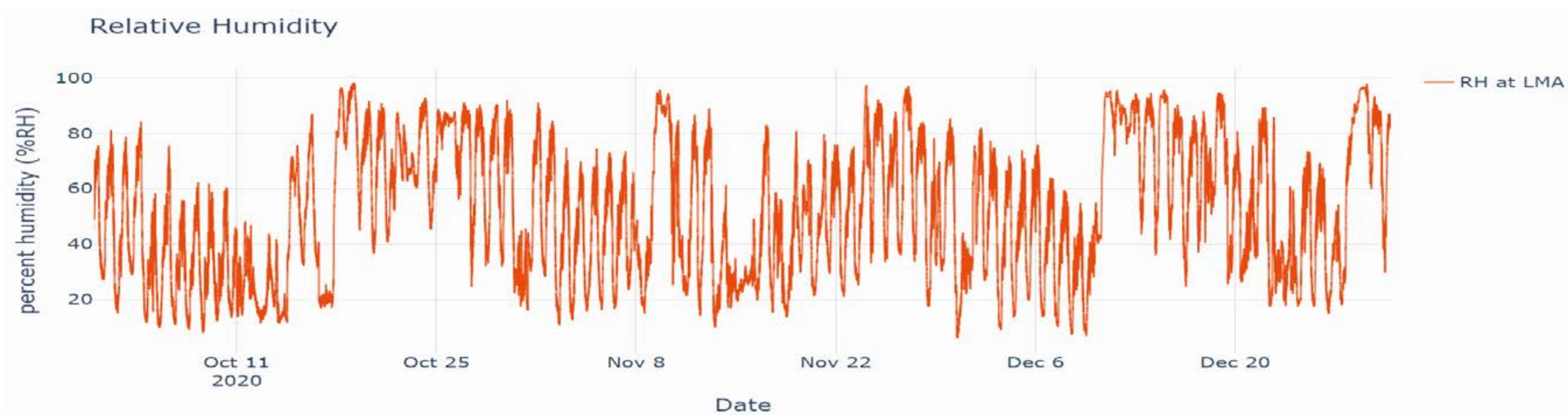

Figure SA2:
LMA humidity record Oct 1 – Dec 31, 2020.

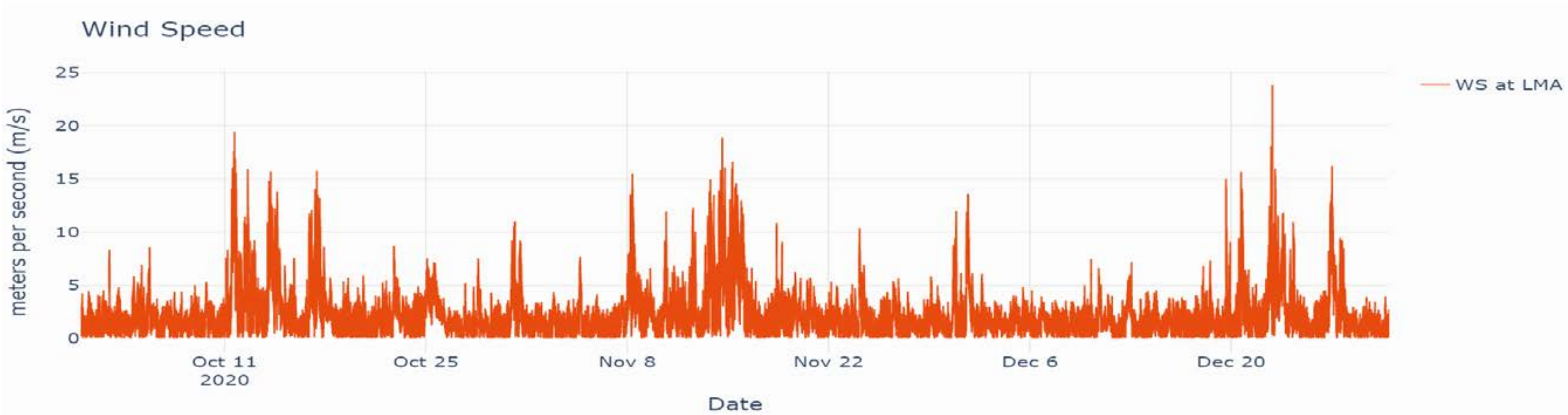

Figure SA3:
LMA wind speed record Oct 1 – Dec 31, 2020.

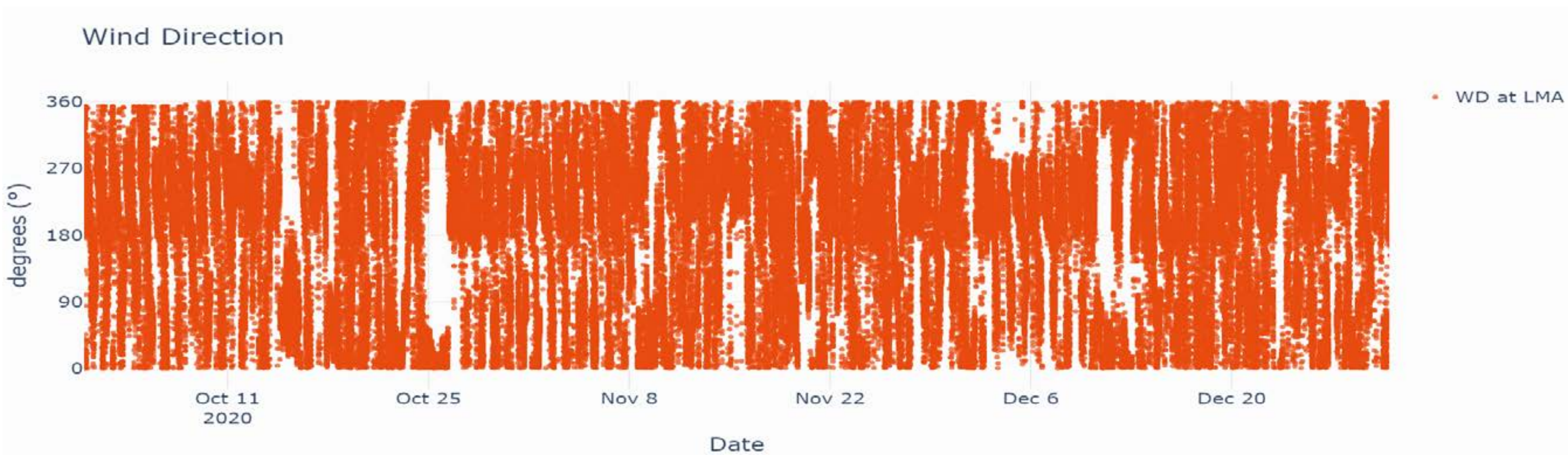

Figure SA4:
LMA wind direction record Oct 1 – Dec 31, 2020.

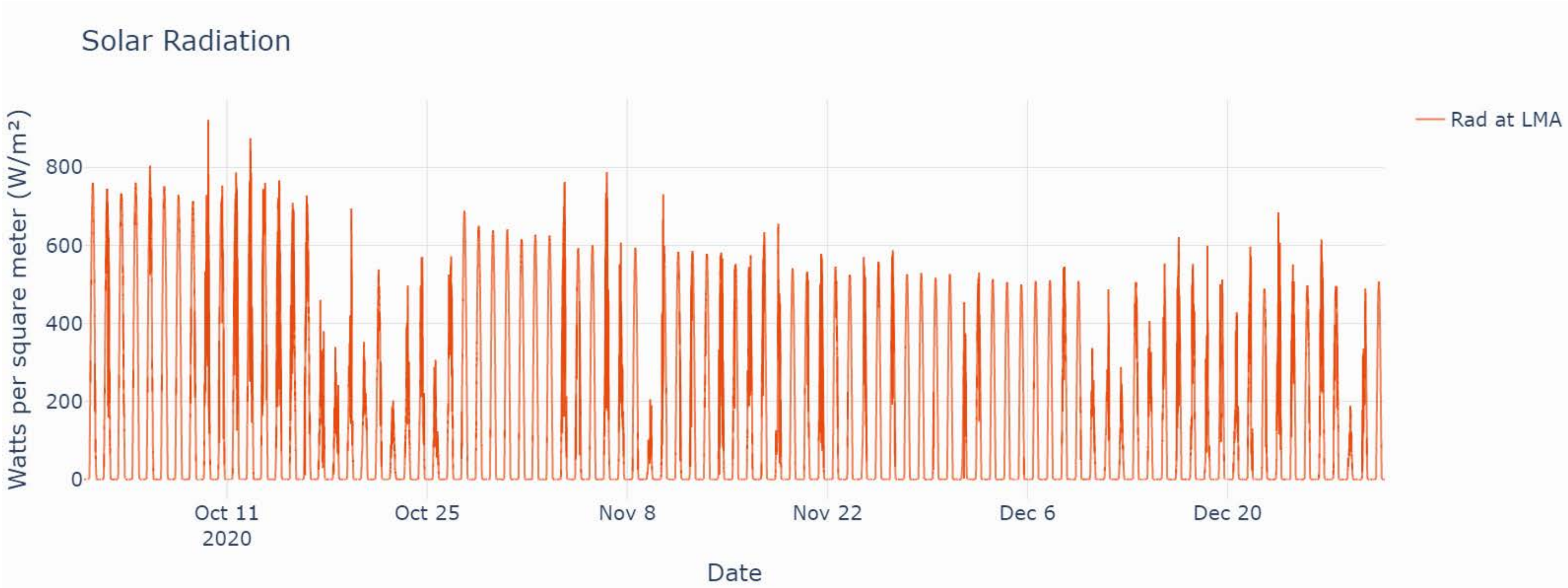

Figure SA5:
LMA solar radiation record Oct 1 – Dec 31, 2020.

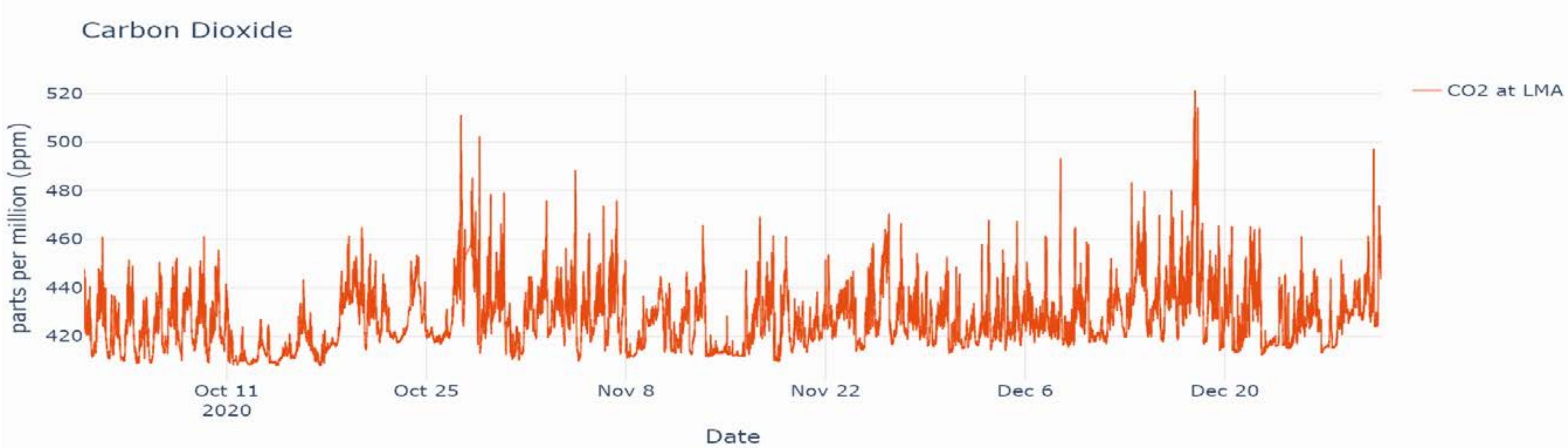

Figure SA6:
LMA CO_2 record Oct 1 – Dec 31, 2020.

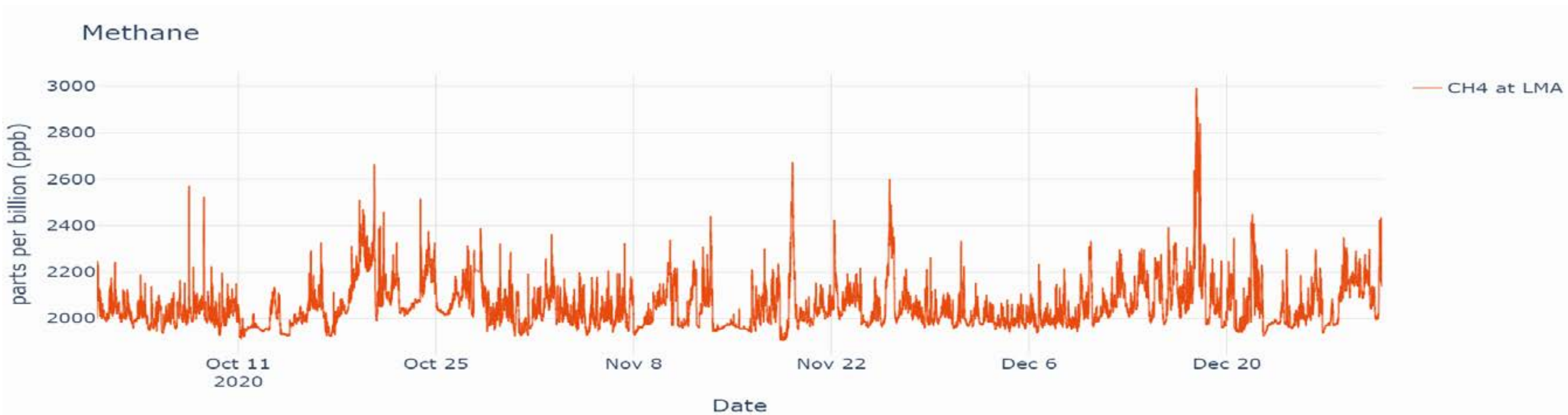

Figure SA7:
LMA CH_4 record January July 1 – September 30, 2020.

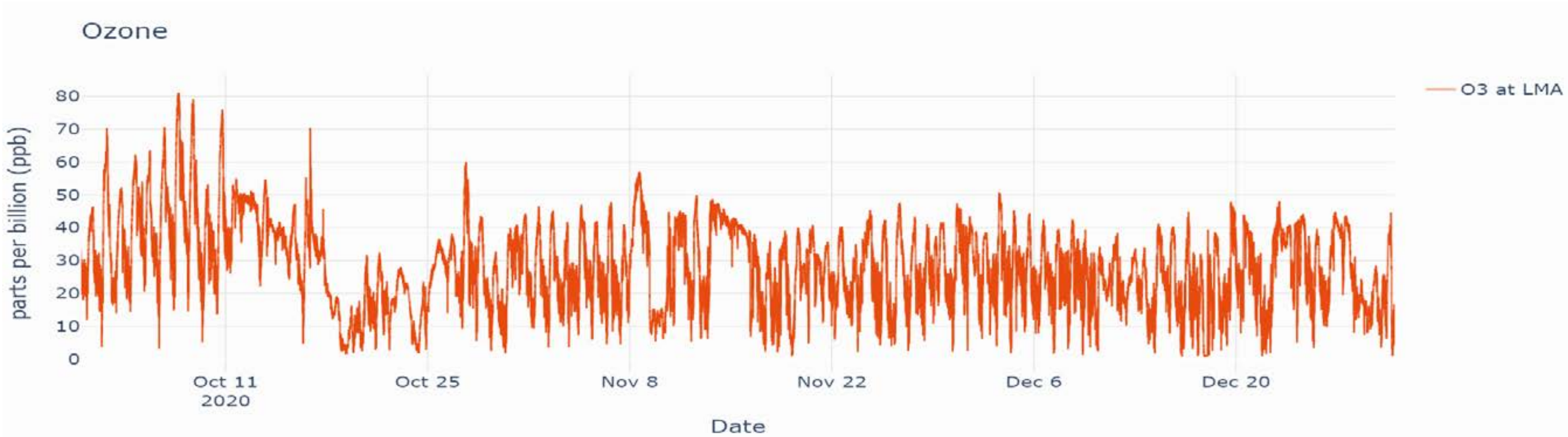

Figure SA8:
LMA ozone record Oct 1 – Dec 31, 2020.

Figure SA9:
LMA ozone 8-hour running average Oct 1 – Dec 31, 2020.

Supplement B

Preliminary Data LUR Quarter 4, 2020

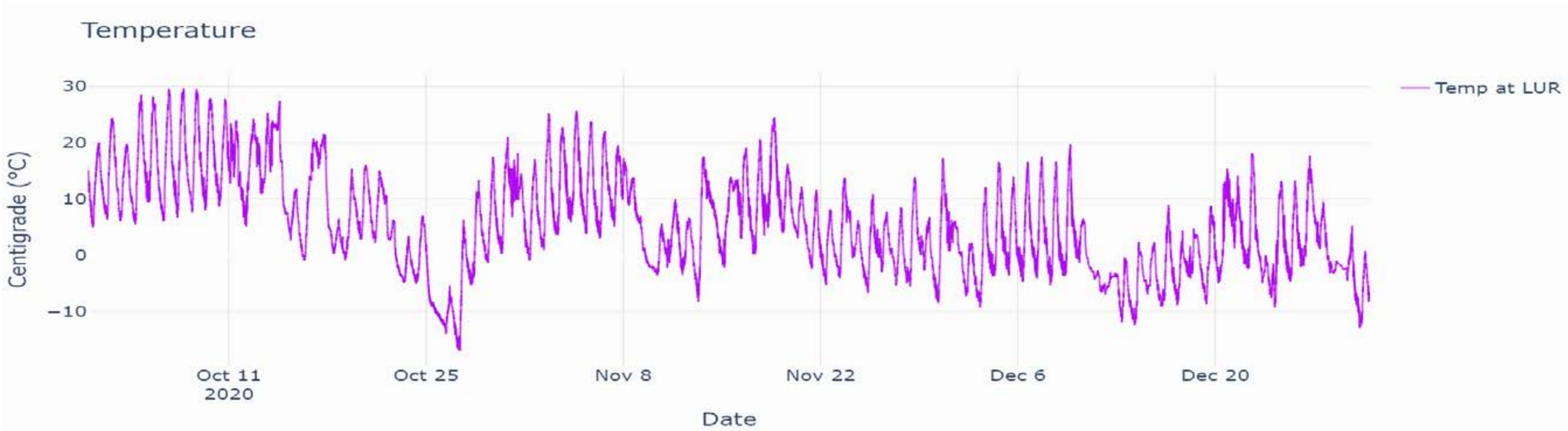

Figure SB1:
LUR temperature record Oct 1 – Dec 31, 2020.

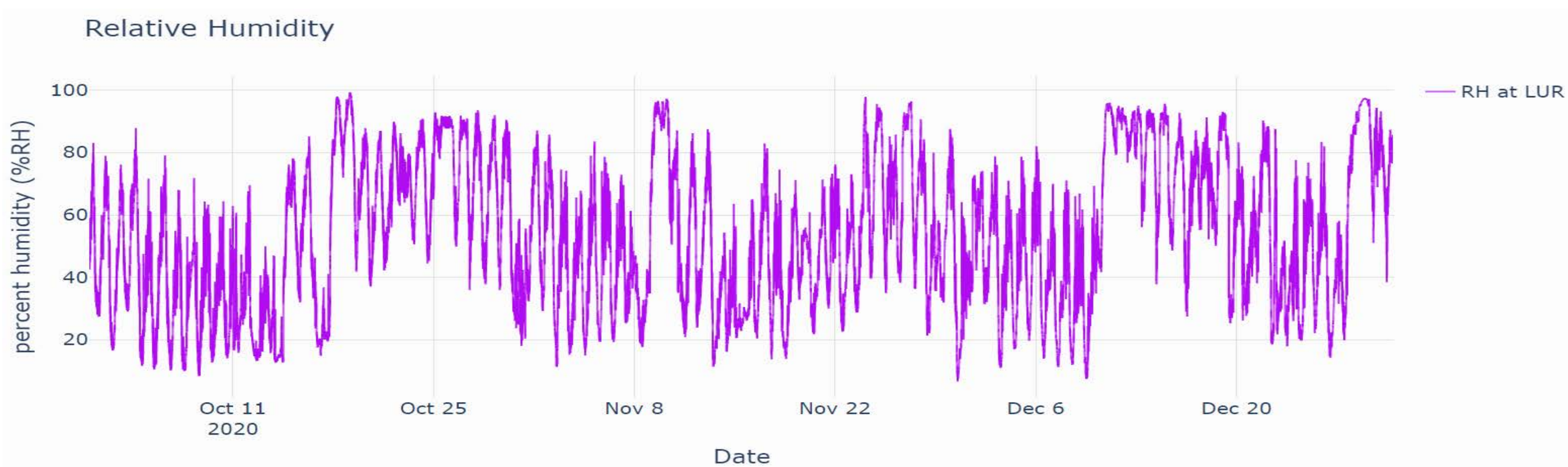

Figure SB2:
LUR humidity record Oct 1 – Dec 31, 2020.

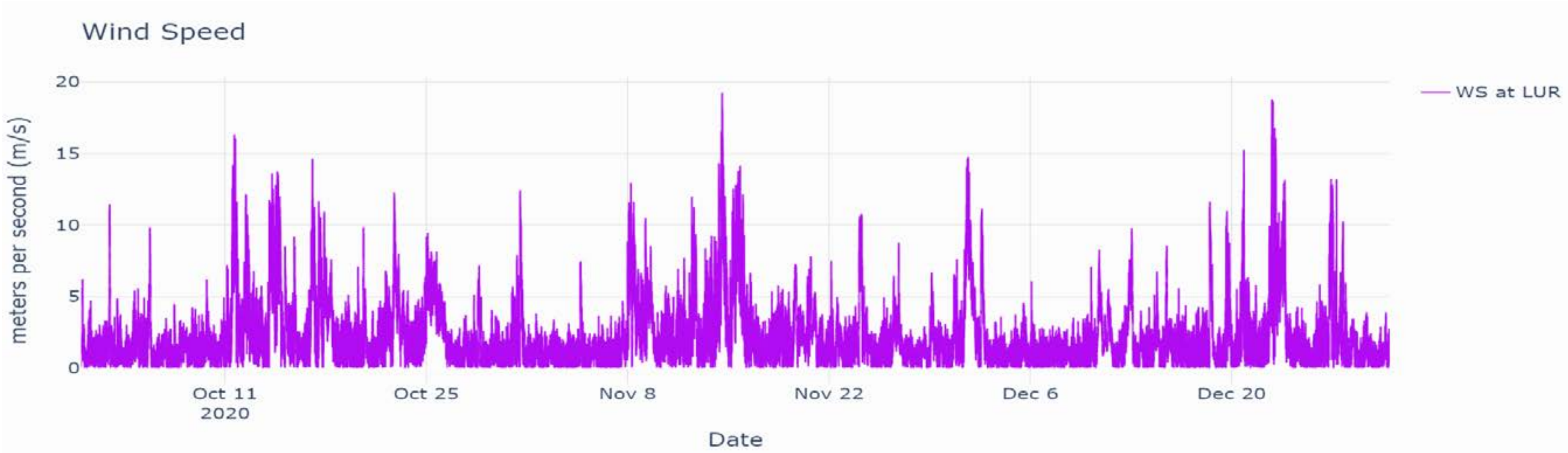

Figure SB3:
LUR wind speed record Oct 1 – Dec 31, 2020.

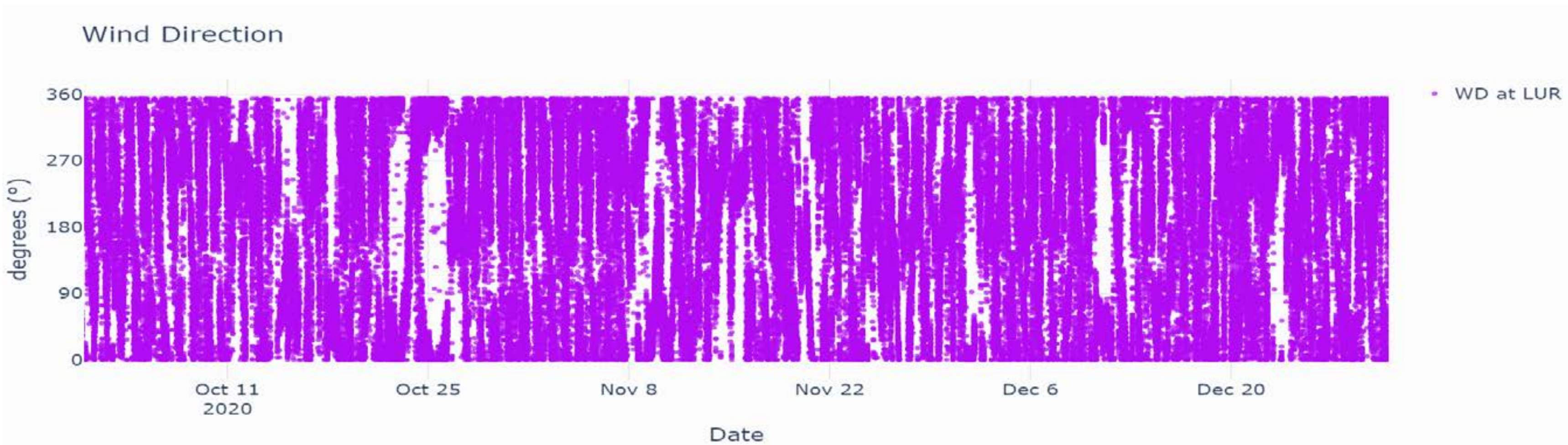

Figure SB4:
LUR wind direction record Oct 1 – Dec 31, 2020.

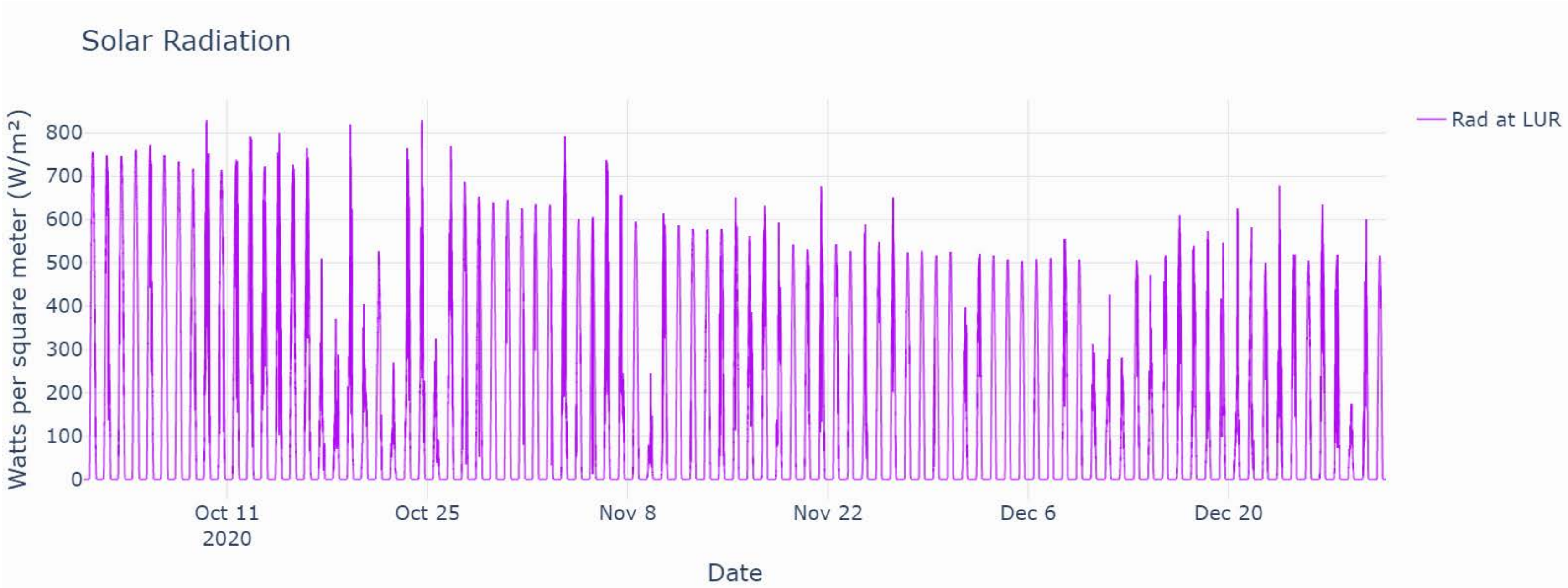

Figure SB5:
LUR solar radiation record Oct 1 – Dec 31, 2020.

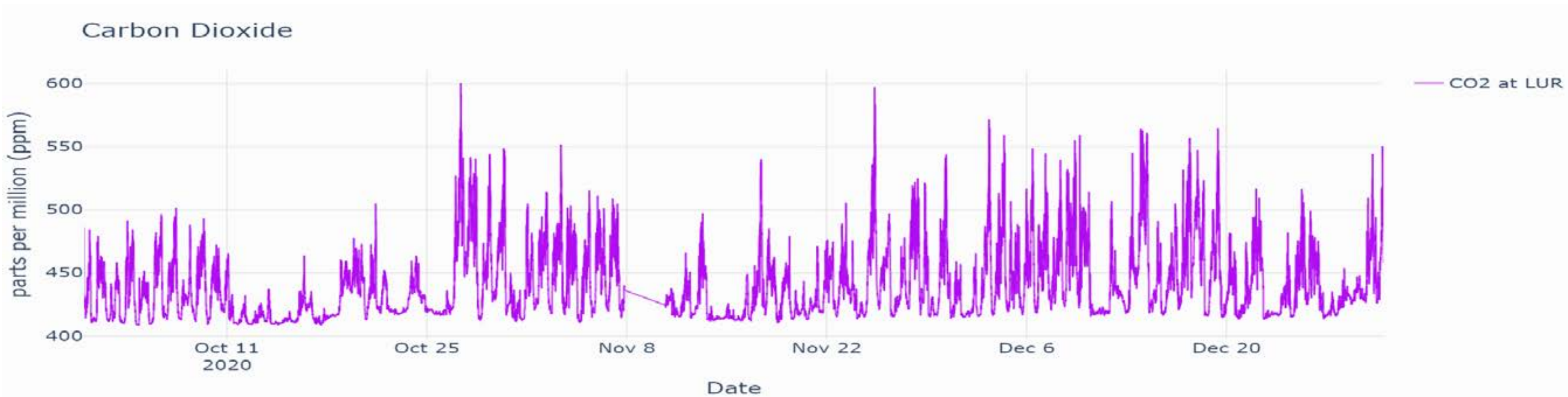

Figure SB6:
LUR CO_2 record Oct 1 – Dec 31, 2020.

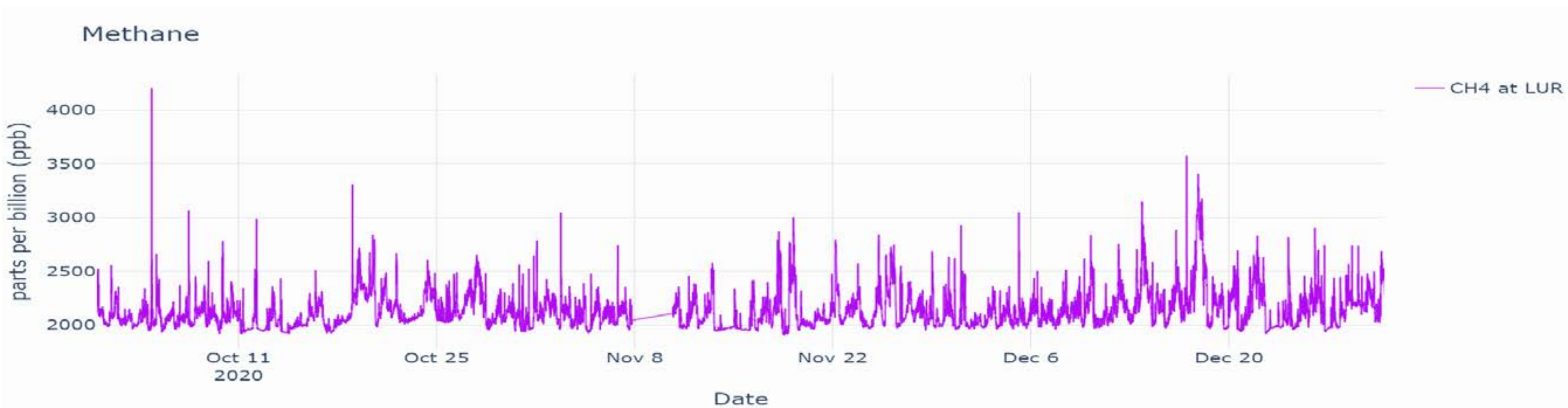

Figure SB7:
LUR methane record Oct 1 – Dec 31, 2020.

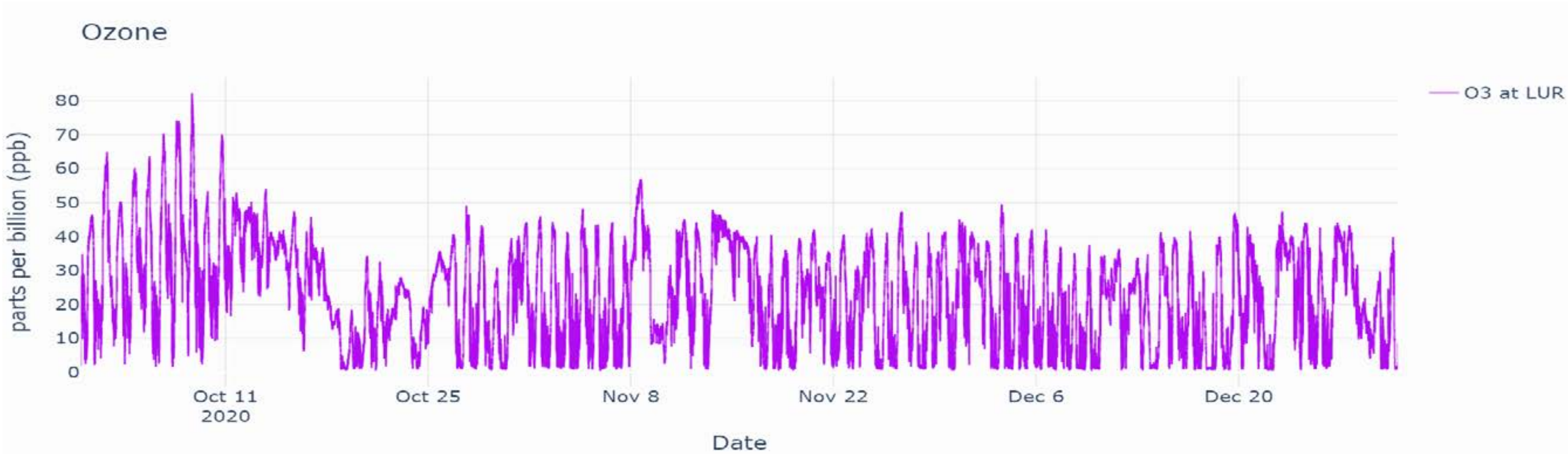

Figure SB8:
LUR ozone record Oct 1 – Dec 31, 2020.

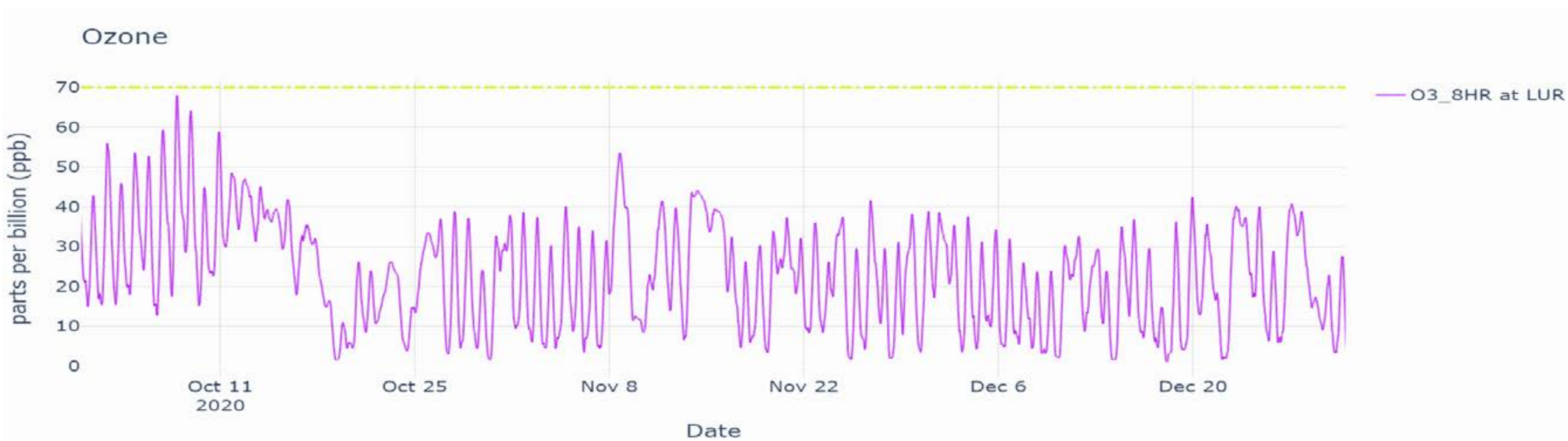

Figure SB9:
LUR ozone 8-hour running average record Oct 1 – Dec 31, 2020.

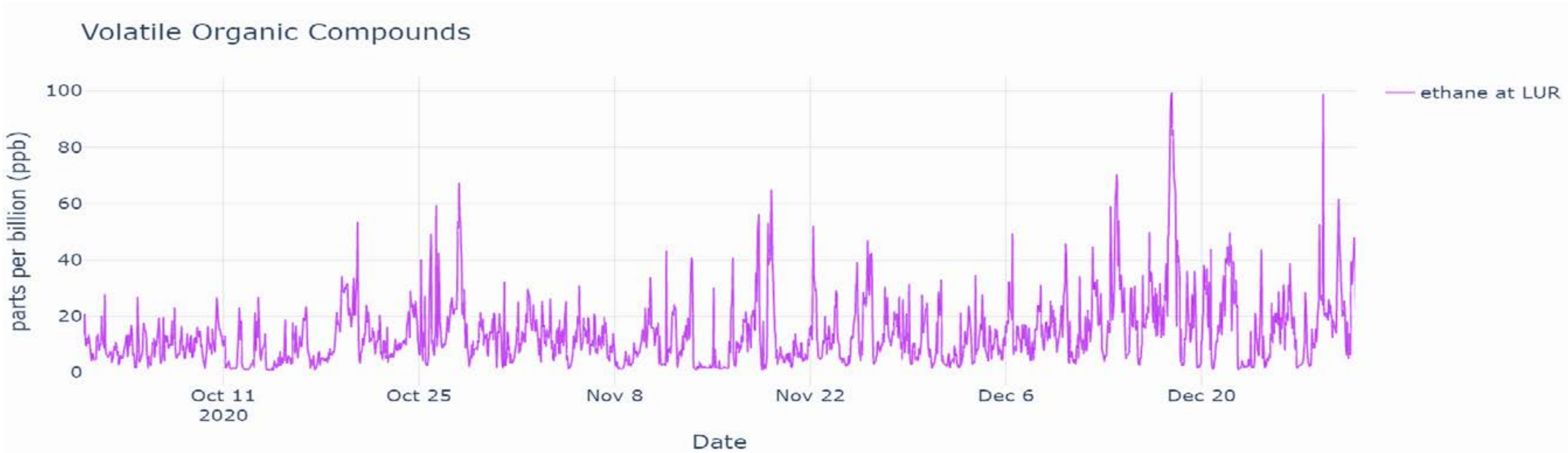

Figure SB10:
LUR ethane record Oct 1 – Dec 31, 2020.

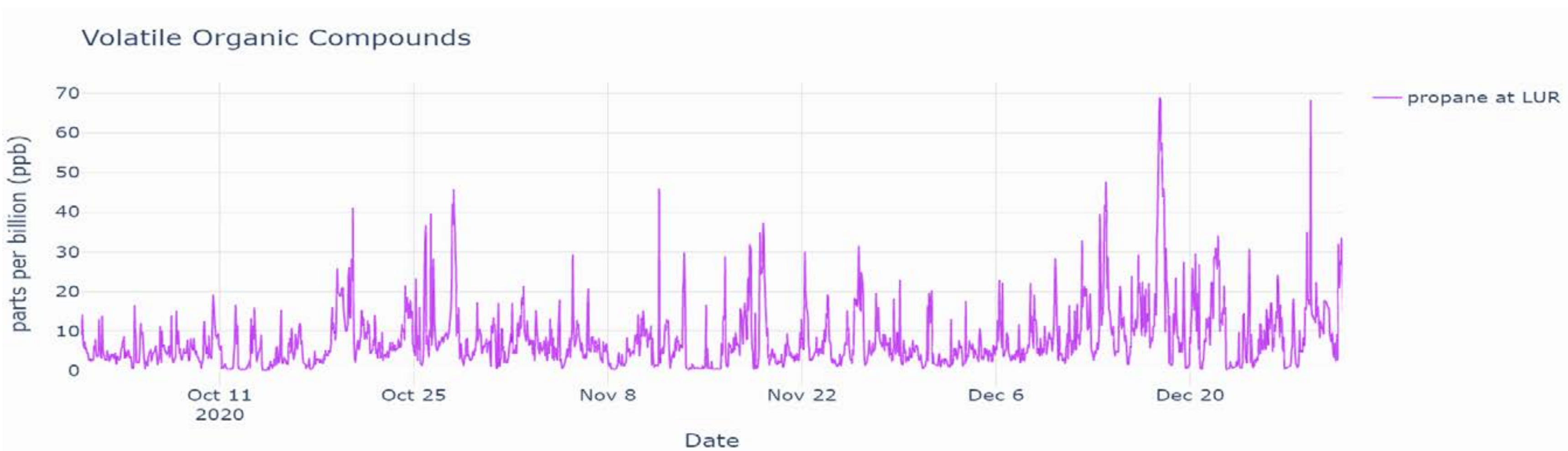

Figure SB11:
LUR propane record Oct 1 – Dec 31, 2020.

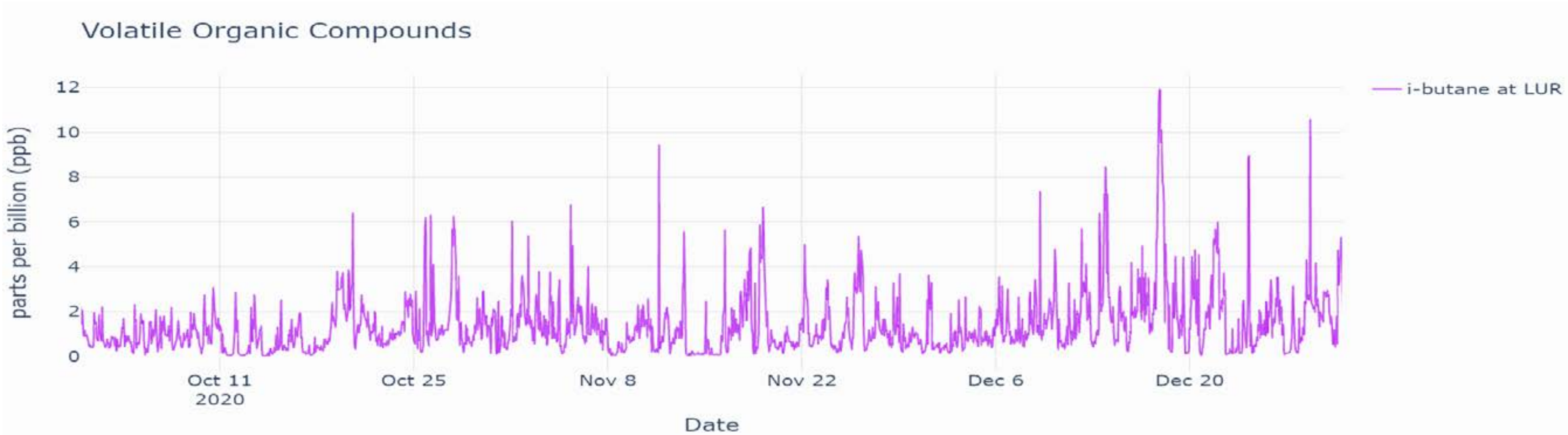

Figure SB12:
LUR i-butane record Oct 1 – Dec 31, 2020.

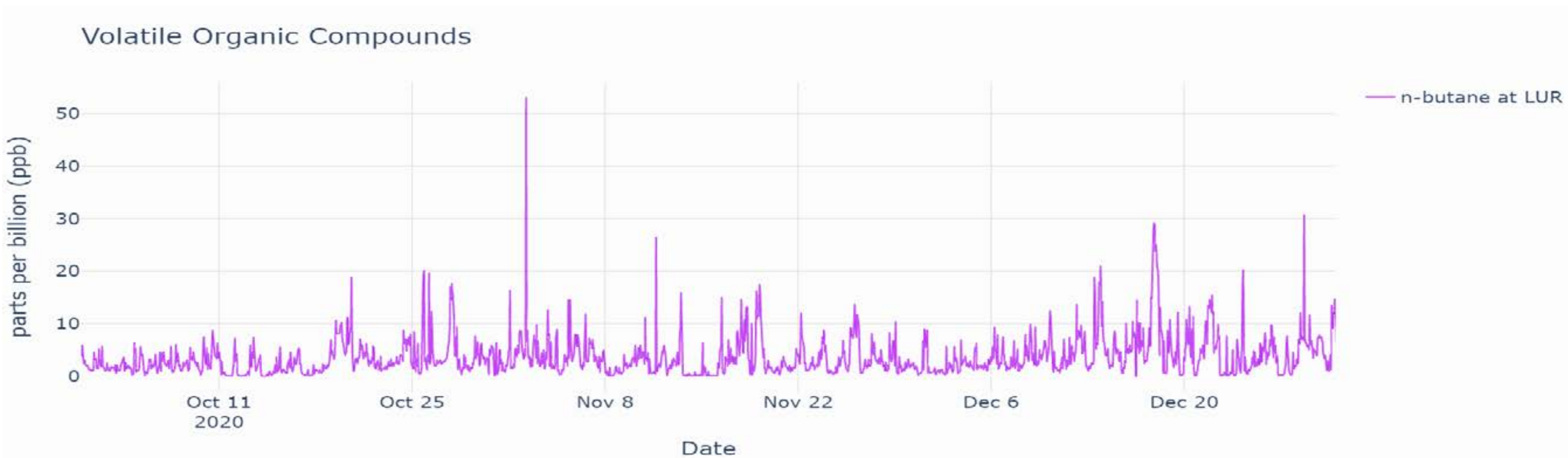

Figure SB13:
LUR n-butane record Oct 1 – Dec 31, 2020.

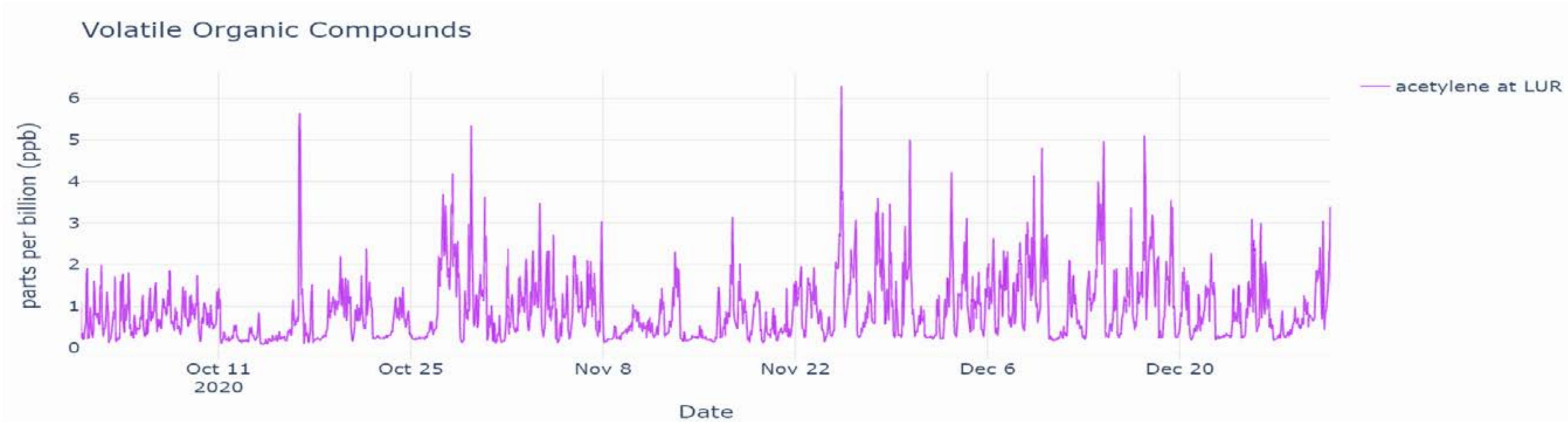

Figure SB14:
LUR acetylene record Oct 1 – Dec 31, 2020.

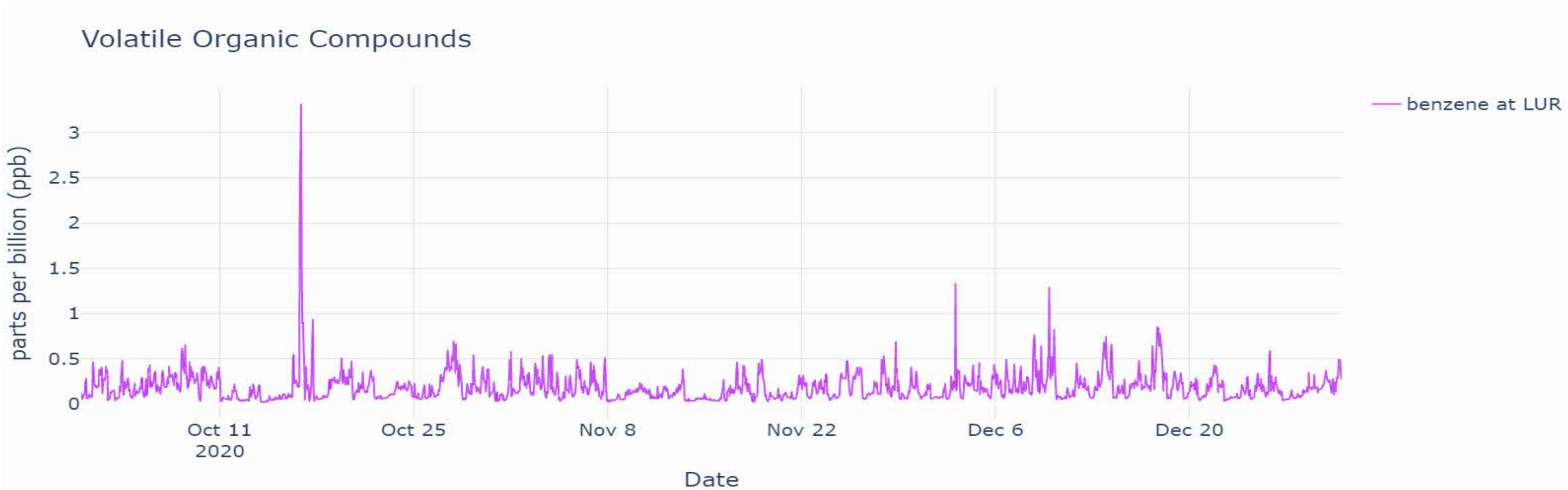

Figure SB15:
LUR benzene record Oct 1 – Dec 31, 2020.

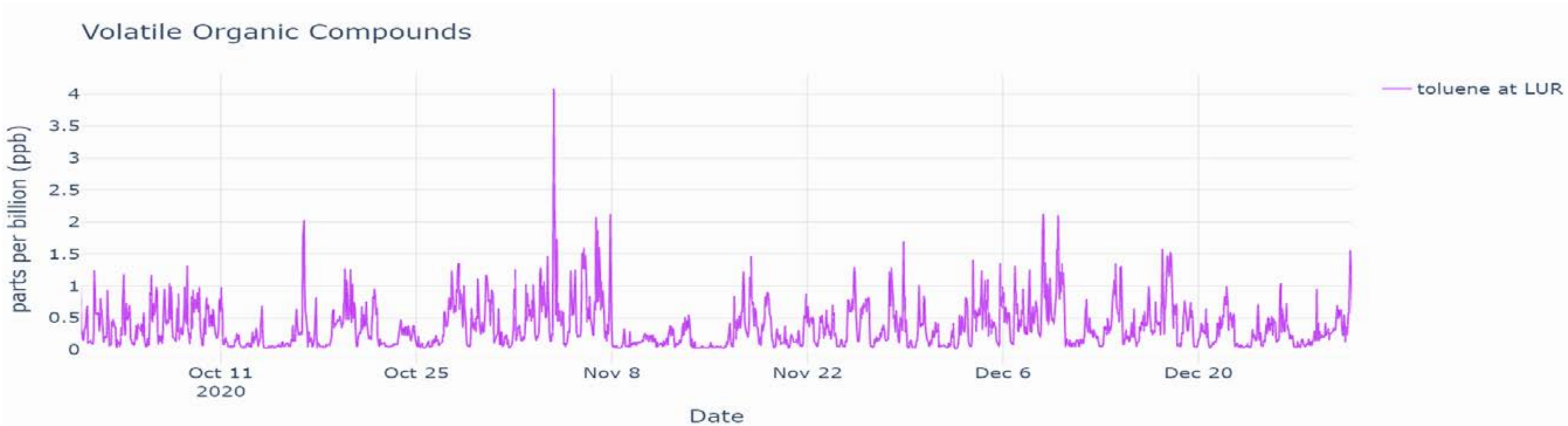

Figure SB16:
LUR toluene record Oct 1 – Dec 31, 2020.

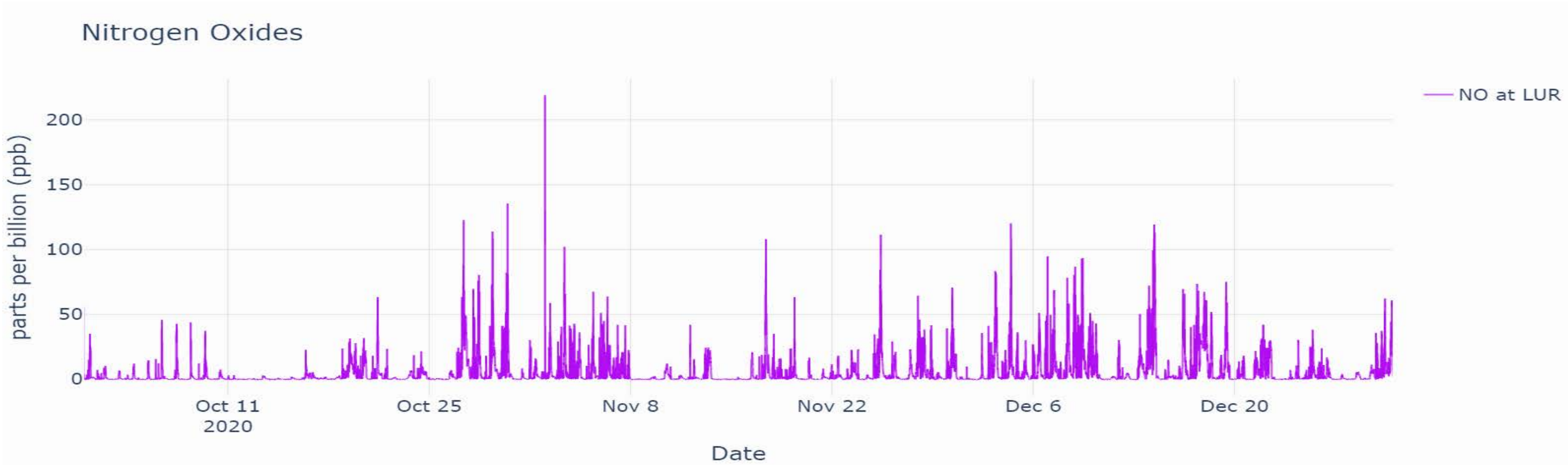

Figure SB17:
LUR nitric oxide record Oct 1 – Dec 31, 2020.

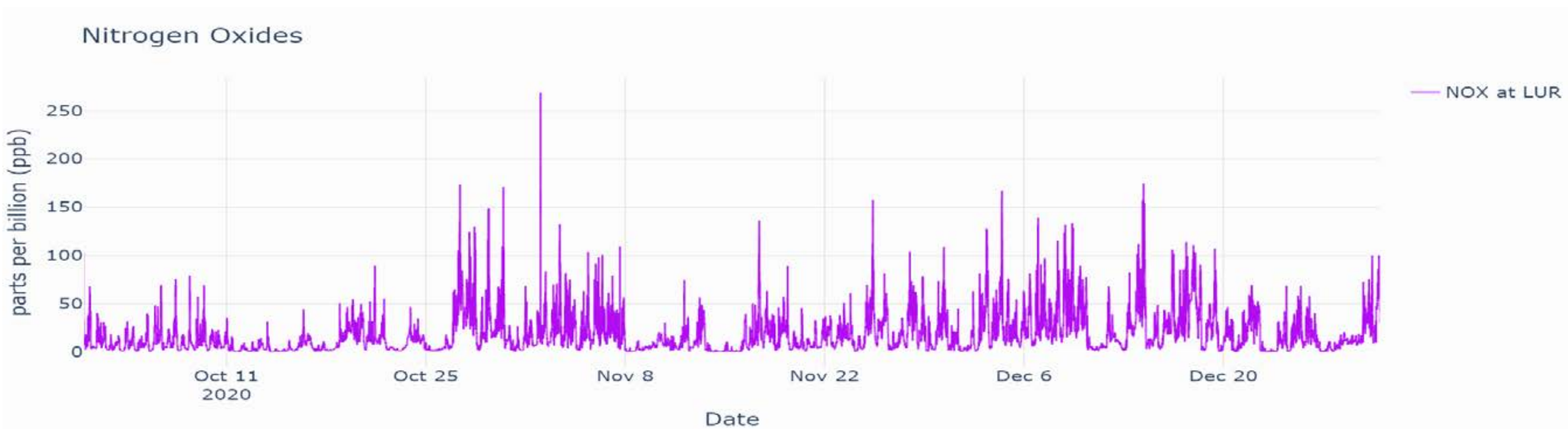

Figure SB18:
LUR nitrogen oxides record Oct 1 – Dec 31, 2020.

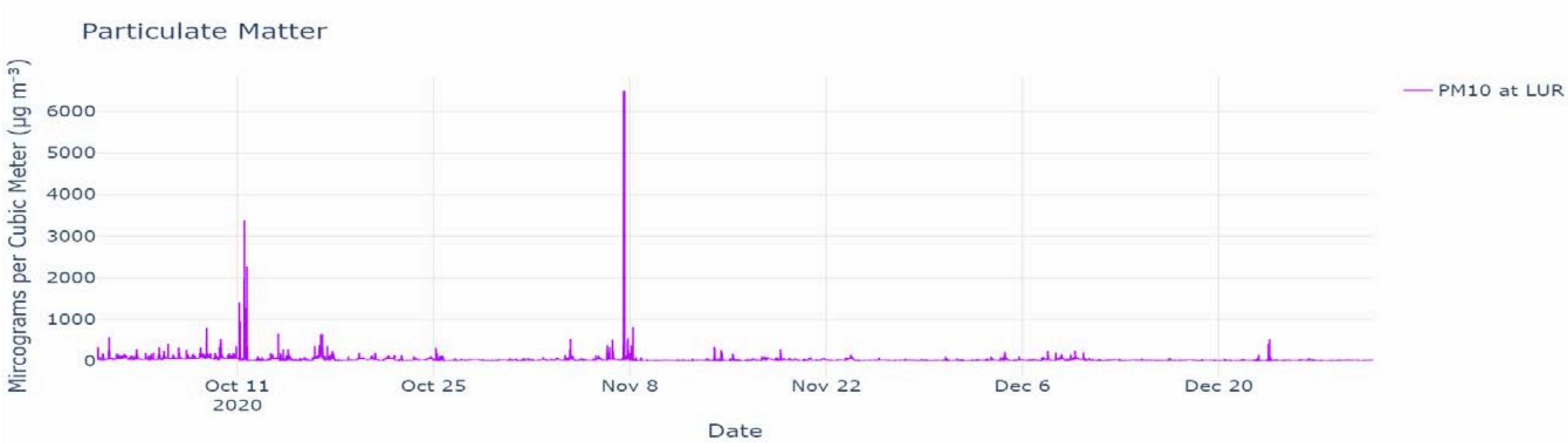

Figure SB19:
LUR coarse particulate matter PM_{10} record for Oct 1 – Dec 31, 2020.

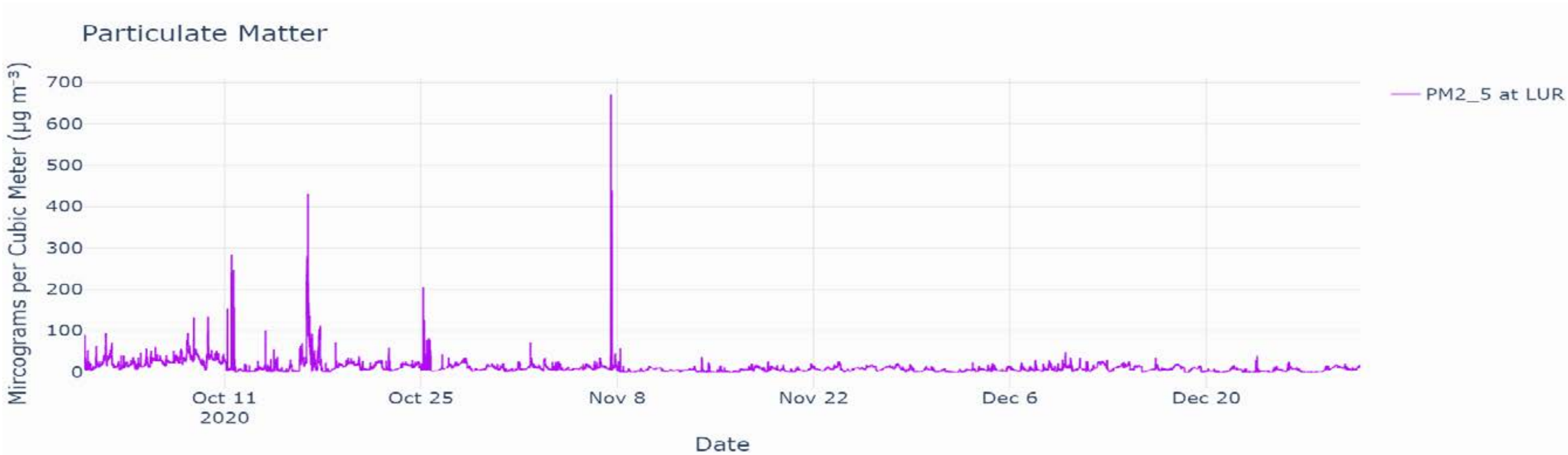

Figure SB20:
LUR fine particulate matter $PM_{2.5}$ record for Oct 1 – Dec 31, 2020.

Figure SB21:
LUR 24-hour averaged fine particulate matter $PM_{2.5}$ record for Oct 1 – Dec 31, 2020.

Supplement C

Comparison of Preliminary Data LMA & LUR 2020

Figure SC1:
LMA & LUR Temperature record Oct 1 – Dec 31, 2020.

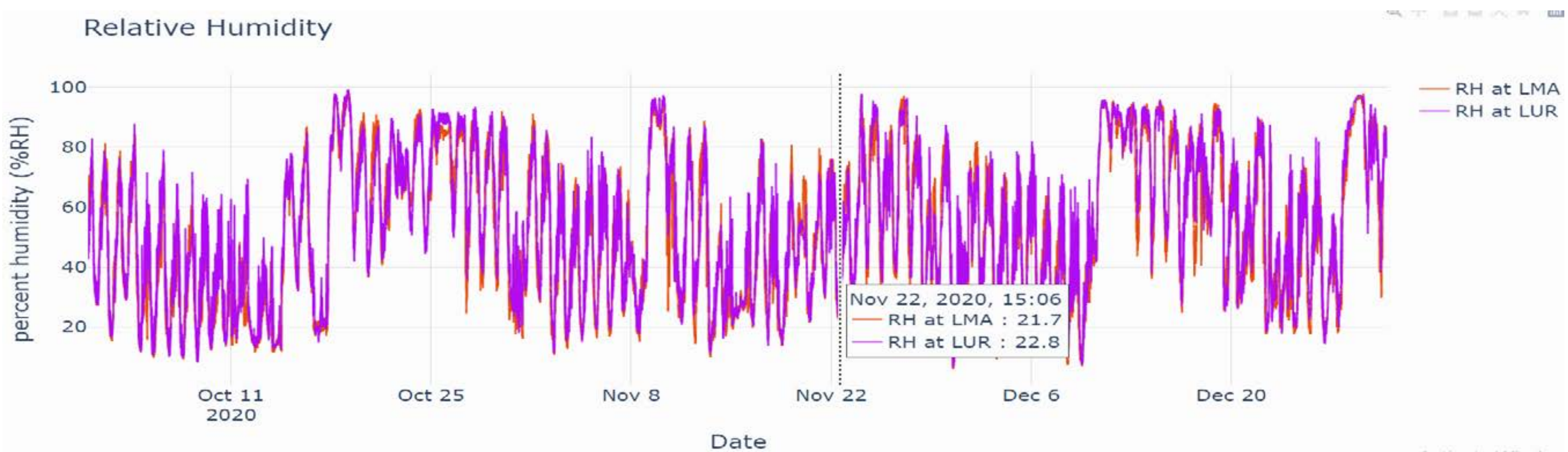

Figure SC2:
LMA & LUR relative humidity record September Oct 1 – Dec 31, 2020.

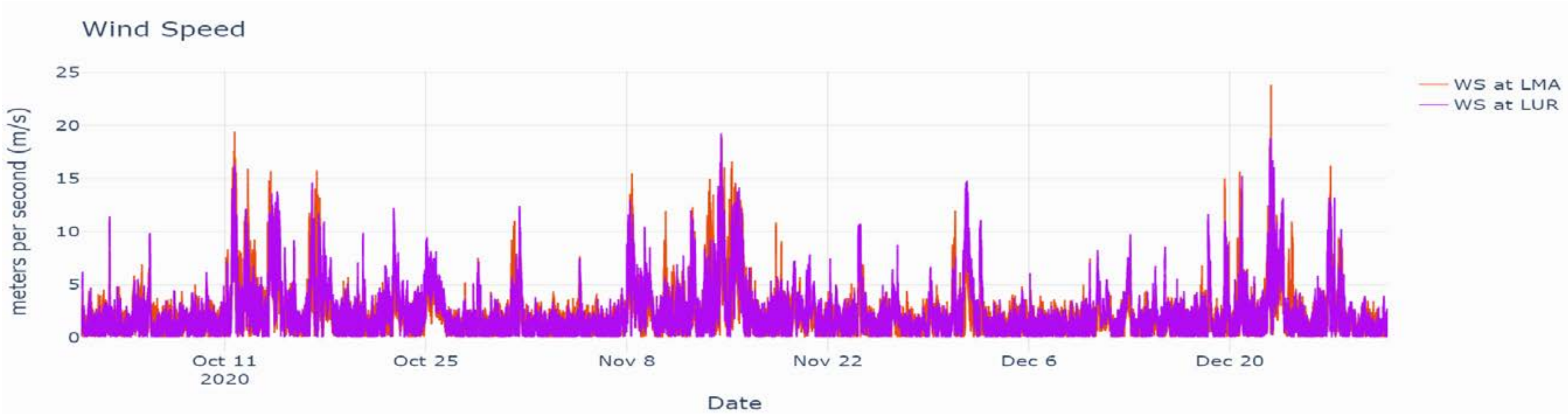

Figure SC3:
LMA & LUR wind speed record Oct 1 – Dec 31, 2020.

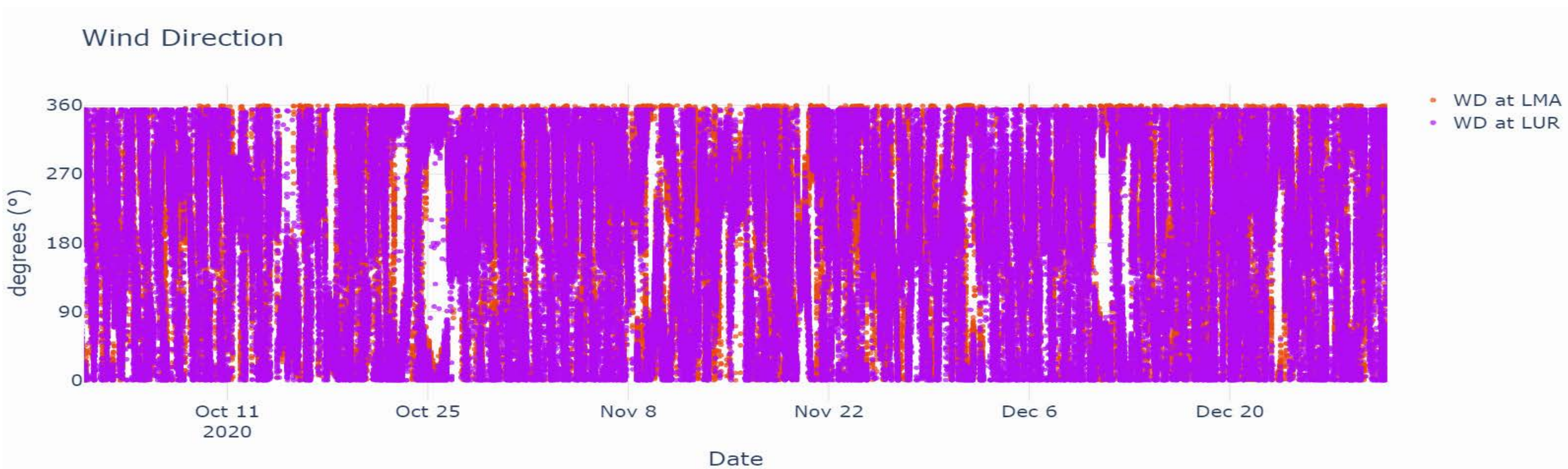

Figure SC4:
LMA & LUR wind direction record Oct 1 – Dec 31, 2020.

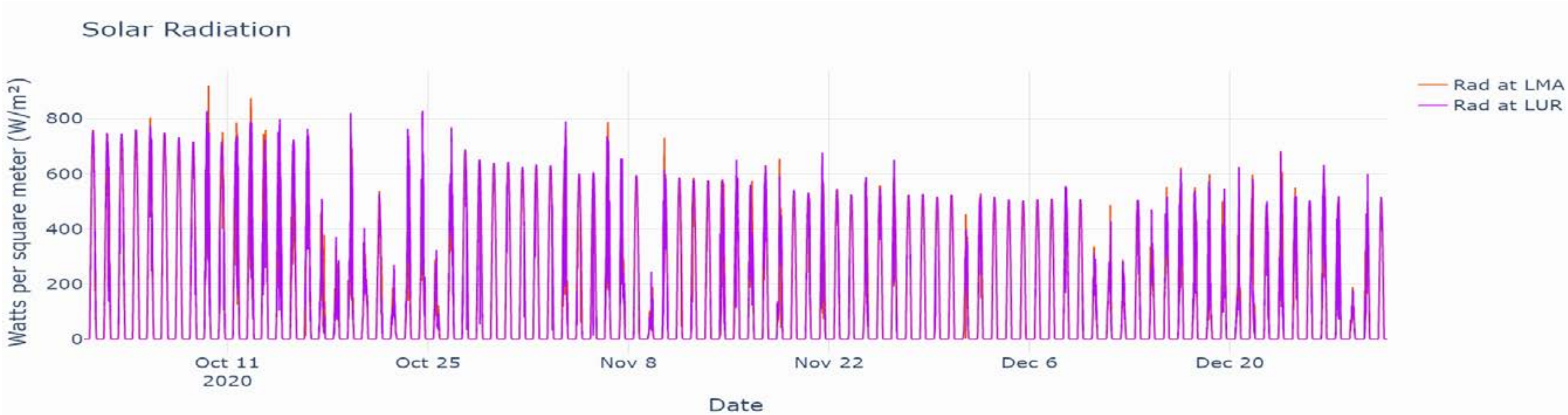

Figure SC5:
LMA & LUR solar radiation record Oct 1 – Dec 31, 2020.

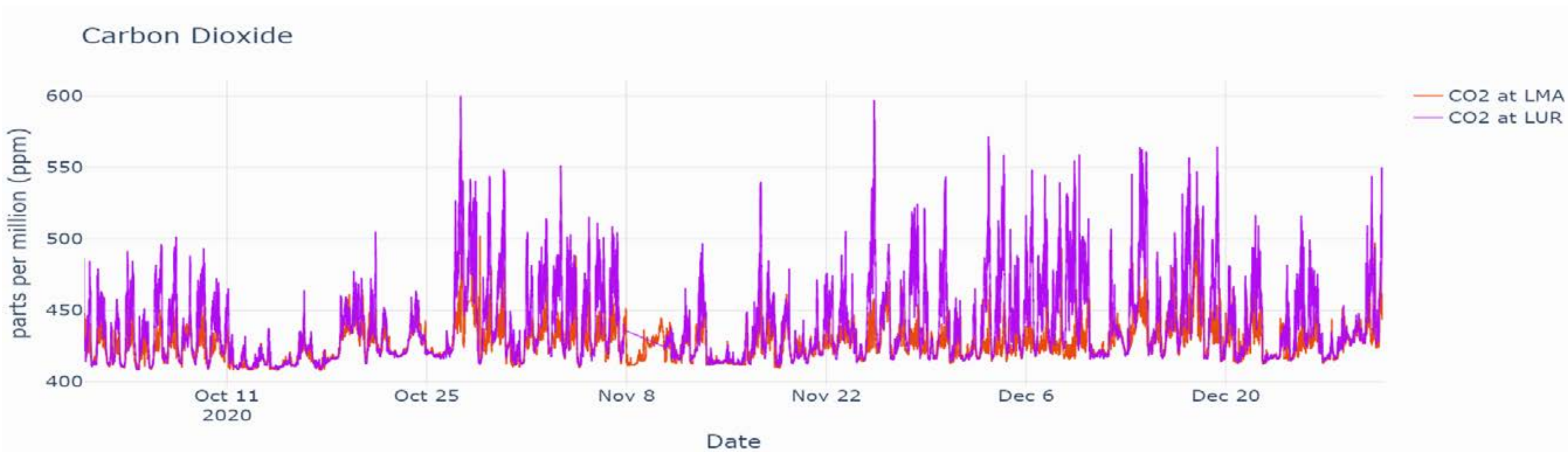

Figure SC6:
LMA & LUR CO_2 record September Oct 1 – Dec 31, 2020.

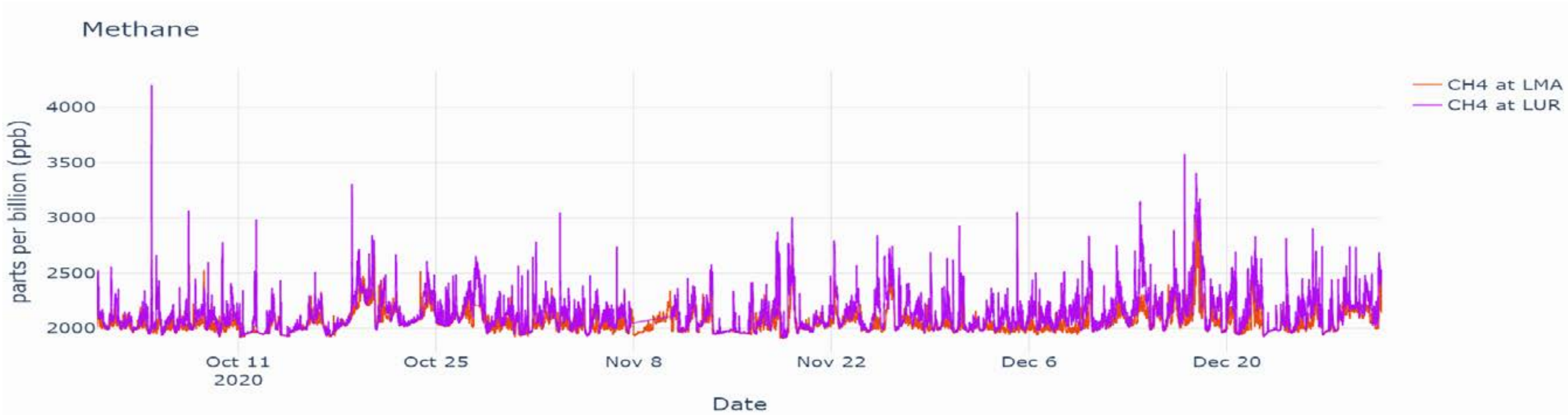

Figure SC7:
LMA & LUR methane record Oct 1 – Dec 31, 2020.

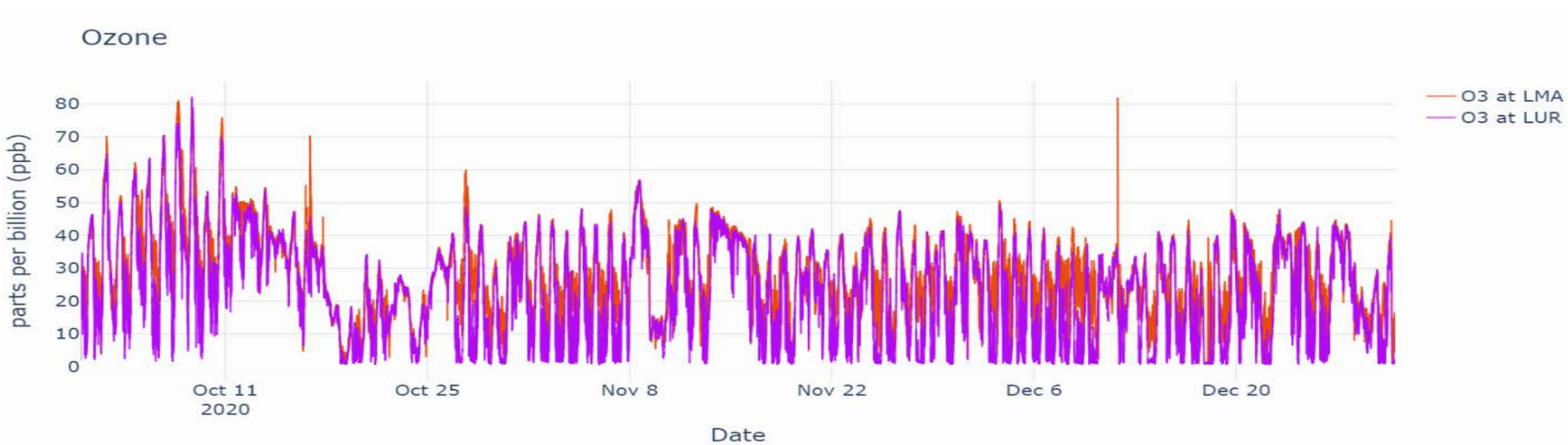

Figure SC8:
LMA & LUR ozone record Oct 1 – Dec 31, 2020.